A pair of dopaminergic neurons DAN-c1 mediate *Drosophila* larval aversive olfactory learning through D2-like receptors

Cheng Qi, Cheng Qian[#], Emma Steijvers[#], Robert A. Colvin, Daewoo Lee*

Department of Biological Sciences, Ohio University, Athens, OH 45701, USA

*Correspondence: leed1@ohio.edu (DL)

[#]Present address:
School of Medicine, Johns Hopkins University, Baltimore, Maryland 21205, USA (CQ);
Department of Physiology, Development and Neuroscience, University of Cambridge, Cambridge CB2 3EL, UK (ES)

Abstract

The intricate relationship between the dopaminergic system and olfactory associative learning in *Drosophila* has been an intense scientific inquiry. Leveraging the formidable genetic tools, we conducted a screening of 57 dopaminergic drivers, leading to the discovery of DAN-c1 driver, uniquely targeting a pair of dopaminergic neurons (DAN) in the larval brain. While the involvement of excitatory D1-like receptors is well-established, the role of D2-like receptors (D2Rs) remains underexplored. Our investigation reveals the expression of D2Rs in both DANs and the mushroom body (MB) of third instar larval brains. Silencing D2Rs in DAN-c1 via microRNA disrupts aversive learning, further supported by optogenetic activation of DAN-c1 during training, affirming the inhibitory role of D2R autoreceptor. Intriguingly, D2R knockdown in the MB impairs both appetitive and aversive learning. These findings elucidate the distinct contributions of D2Rs in diverse brain structures, providing novel insights into the molecular mechanisms governing associative learning in *Drosophila* larvae.

Key Words:

Drosophila larval aversive learning, D2R, DAN-c1, mushroom body, thermogenetics, optogenetics.

36 **Introduction**

37 Learning defines a behavioral change that results from acquiring information about the
38 environment, and memory refers to the process by which the information is encoded, stored,
39 and later retrieved. Learning and memory forms the basis for higher brain functions, including
40 cognition and decision making, which shapes our individuality[1]. On the cellular and physiological
41 level, learning and memory is achieved by neuroplastic changes in circuits, including neuronal
42 excitability and synaptic plasticity. Usually distinct types of neurotransmitters, such as dopamine,
43 modulate these changes.

44 Dopamine (DA) plays an important role in many mammalian brain functions, including
45 motor functions, motivation, reinforcement, addiction, and learning and memory[2-4].
46 Dopaminergic neurons (DAN) are mainly located in the mesencephalon: DANs in the substantia
47 nigra (SN) are responsible for motor functions, while those in the ventral tegmental area (VTA)
48 are important in reward, addiction, learning and memory[3,5]. Dopamine achieves its functions via
49 two families of G protein-coupled receptors (GPCR): excitatory D1-like and inhibitory D2-like
50 receptors[4]. All D1-like receptors are located post-synaptically; in contrast, D2-like receptors both
51 function post-synaptically and play an important presynaptic role, regulating dopamine release
52 through negative feedback[4]. All these receptors are important in mammalian associative
53 learning[6,7]. D1-like receptors elevate intracellular cAMP by activating adenylyl cyclase (AC) via
54 $G\alpha_s$, while D2-like receptors repress cAMP by inhibiting AC via $G\alpha_{i/o}$. cAMP activates protein
55 kinase A (PKA), leading to the phosphorylation of DARPP-32 (dopamine and cyclic AMP-regulated
56 phosphoprotein, 32kDa), ion channels, and CREB (cAMP response element-binding protein). In
57 addition, dopamine receptors also activate the PLC-PKC, MAPK, and CaMKII pathways[2-4,8-10].

58 Although mammalian studies reveal mechanisms more relevant to human beings, the
59 complexity of the nervous system impedes our understanding about the basic or more universal
60 principles of learning and memory applicable generally to all nervous systems[11]. With a simple
61 central nervous system (CNS) and powerful genetic tools, the fruit fly *Drosophila melanogaster*
62 has become a popular model organism in learning and memory research[12,13]. With conserved
63 genes in dopamine metabolism and signaling[14], as well as fundamental similarities in the
64 olfactory circuitry compared to mammals[15,16], *Drosophila* can perform olfactory associative
65 learning in both larvae[17-19] and adults[20-24]. Olfactory associative learning is a type of classical
66 conditioning in which flies are trained under positive or negative reinforcement paired with an
67 odorant. Different from the naïve reaction to the odorant, flies approach the odorant after being
68 trained with rewards (e.g., sucrose; appetitive)[21], but avoid the odorant when trained with
69 punishments (e.g., electric shock, bitter taste chemicals; aversive)[20]. Several genes related to the
70 cAMP-PKA signaling pathway, including *dunce* (*dnc*)[25] and *rutabaga* (*rut*)[21], are expressed in the
71 mushroom body (a center for *Drosophila* learning and memory) in both larval and adult brains[26,27].
72 Mutations of these genes lead to learning deficiencies, indicating their roles in larval[17,18] and adult
73 olfactory learning[21,25].
74 *Drosophila* larvae offer several advantages for studying olfactory learning compared to
75 adults. Notably, compared to neural circuits underlying olfactory learning, their simpler neural
76 circuitry[28], characterized by fewer olfactory receptor neurons (ORNs)[29], projection neurons
77 (PNs)[30], mushroom body neurons (MBNs)[31], and dopaminergic neurons (DANs)[32], facilitates the
78 elucidation of underlying mechanisms. Additionally, larvae exhibit simpler behavioral patterns,
79 facilitating experimental manipulations and observations. Furthermore, their translucent cuticles

80 enable convenient application of techniques such as optogenetics[33], further enhancing the
81 experimental versatility of larval studies.

82 Like in mammalian brains, dopamine achieves its functions via four dopamine receptors in
83 flies, two D1-like receptors dDA1[34] (or Dop1R1) and DAMB[35] (or Dop1R2), one D2-like receptor
84 D2R[36] (or Dop2R), and one non-canonical receptor DopEcR[14,37]. dDA1 is mainly found in the
85 mushroom body[38,39] and is necessary for appetitive and aversive olfactory learning in larvae[39]
86 and adults[40]. D2R in the adult mushroom body is necessary for anesthesia-resistant memory[41].
87 In addition, D2R in GABAergic anterior paired lateral (APL) neurons is known to secure aversive
88 conditioning in adult flies[42]. Although D2R expression has been reported in the ventral nerve
89 cord[43], neither its expression in larval brains, nor its functions in larval olfactory learning have
90 been investigated.

91 By using a GFP-tagged D2R strain, we detected the expression pattern of D2R in the third-
92 instar larval brain, specifically in dopaminergic and mushroom body neurons. Knockdown of D2Rs
93 in a pair of DANs, DAN-c1, impaired aversive learning, while knockdown of D2R in mushroom
94 body neurons led to deficits in both aversive and appetitive learning. These results revealed that
95 D2Rs in distinct brain structures mediate different learning tasks. The newly discovered roles of
96 D2R in the larval brain provides new insights into the mechanisms underlying larval associative
97 learning.

98 **Results**

99 **Distinct dopaminergic neurons innervate different compartments of the mushroom body.**

100 The connectome of larval learning circuitries has been investigated in both first- and third-
101 instar larvae[28,44]. The mushroom body serves as a primary learning center in *Drosophila*, which is
102 composed by αβ, α'β', and γ neurons in adult brains[45]. In larvae, axons from γ neurons bifurcate
103 and form the vertical and medial lobes, as αβ and α'β' neurons are not mature[31,46,47]. These lobes
104 are divided into 11 compartments (refer to Figure 1) based on the coverage of neurites from both
105 mushroom body extrinsic neurons (MBEN) and mushroom body output neurons (MBON)[28].
106 Around 21 dopaminergic neurons are found in each third-instar brain hemisphere, and
107 categorized into 4 clusters: DM1 (dorsomedial), pPAM (primary protocerebral anterior medial,
108 or DM2)[48], DL1 (dorsolateral), and DL2[32]. DL1 neurons project to the vertical lobe[39], while pPAM
109 neurons innervate the medial lobe[48] (refer to Figure 1a-c).

110 In this study, we wanted to functionally identify individual DANs that mediate larval olfactory
111 learning. The first step was to search for DAN-specific driver strains that mark a few dopaminergic
112 neurons, which subsequently can be used to target genetic manipulations of corresponding
113 neurons. A total of 57 driver strains identifying dopaminergic neurons were screened in this study
114 (Table 1). These strains were chosen based on previous studies, either identifying a pair of
115 dopaminergic neurons in larvae, or identifying only several in adult brains and indicating the
116 potential of identifying a pair of DANs in larvae. TH-GAL4, a traditional dopaminergic neuronal
117 driver[49], identifies all dopaminergic neurons except those in pPAM (Figure 1d, Figure S1a). Split-
118 GFP reconstitution across synaptic partners (GRASP) technique was used to investigate the
119 "direct" synaptic connections from DANs to the mushroom body (MB), in which portions of GFP

120 were specifically expressed in corresponding neurons (Figure S2d)[50]. GRASP results showed
121 neurons under TH-GAL4 formed synapses in the vertical lobe and lower peduncle (white dash
122 lines in Figure 1d'), consistent with previous electron microscopy data[44]. We found three DAN
123 driver strains that identify a pair of dopaminergic neurons in the third-instar larval brain. DAN
124 driver R76F02-AD;R55C10-DBD identifies a pair of dopaminergic neurons innervating the lower
125 peduncle (LP), which would be DAN-c1 based on previous published nomenclature[28] (Figure 1f).
126 MB296B driver identifies the dopaminergic neurons (DAN-d1) projecting to the lateral appendix
127 (LA) (Figure 1g), as well as many non-dopaminergic neurons. SS1716 driver identifies a pair of
128 dopaminergic neurons forming synapses in the lower vertical lobe (LVL), indicating it is DAN-g1
129 (Figure 1h).

130 In pPAM, R58E02 driver identifies DAN-h1, i1, and j1, innervating the shaft (SHA),
131 intermediate toe (IT) and upper toe (UT) (Figure 1i), and R30G08 driver identifies DAN-h1 and i1
132 (Figure 1j). As described in a previous report[28], SS864 driver identifies DAN-i1, innervating the
133 upper toe (Figure 1l), and SS1757 driver identifies DAN-k1 which innervates the lower toe (LT)
134 (Figure 1m). In contrast, SS1696 driver identifies not only DAN-h1, but also i1 and one DL1 neuron
135 not innervating the mushroom body (Figure 1k).

136 In summary, our results show that five DL1 and four pPAM DANs innervate nine distinct
137 mushroom body compartments in a one-to-one pattern (Figure 1b and c). DL1 neurons innervate
138 the vertical lobe and peduncle, while pPAM neurons project to the medial lobe. The neuronal
139 driver strains screened can be used to investigate the roles of individually identified DANs in larval
140 olfactory learning.

141

142 **Dopamine release from DAN-c1 mediates larval aversive learning.**

143 Dopamine plays an important role during olfactory associative learning in both adults[51,52]
144 and larvae[17,18]. In adults, dopaminergic neurons in PPL1 regulate aversive learning[53-56], while
145 those in PAM mediate reward signals in appetitive learning[57-59]. In larvae, DL1 neurons
146 innervating the vertical lobe and the peduncle are required for aversive learning[18,39], while those
147 in pPAM projecting to the medial lobe are involved in appetitive learning[48].

148 In Figure 1 and Table 1, three driver strains identifying distinct pairs of dopaminergic
149 neurons in DL1 were discovered, which could be candidates to investigate their roles in larval
150 aversive learning. The R76F02-AD;R55C10-DBD strain identifies MB-MP1 in the adult brain[60],
151 which is a dopaminergic neuron involved in adult aversive learning[61]. Based on the analysis with
152 22 brain samples, we observed this driver strain labels one neuron per hemisphere in the third-
153 instar larval brain (Figure 2a-d, Figure S1c, Table S3). Using a UAS-DenMark;UAS-sytGFP strain,
154 its dendrites were labeled with RFP and axonal terminals were marked by GFP. Its dendrites were
155 localized in the dorsomedial protocerebrum (dml), and its axonal terminals located in the lower
156 peduncle of the mushroom body (Figure 2a and c), with GRASP results supporting the existence
157 of synapses in this compartment (Figure 1f'). All these characteristics are consistent with the
158 previously published nomenclature[28], indicating that this pair of neurons are DAN-c1 (Figure 2d),
159 thus, this strain will now be referred to simply as DAN-c1.

160 To reveal the role of DAN-c1 in larval olfactory learning, a single odor learning paradigm and
161 thermogenetic tools were applied[17,18,62]. Compared to those trained with distilled water (DW),
162 control strains of larvae exhibited repulsion to the odorant pentyl acetate (PA) after being
163 trained with quinine (QUI) paired with PA, reflecting aversive learning. In contrast, larvae were

164 attracted to PA after being trained with sucrose (SUC) paired with PA, reflecting appetitive
165 learning. The extent of repulsion or attraction was represented with a response index (R.I.) that
166 is compared to the DW group (Figure 2e; For further details, refer to the **Materials and Methods**
167 section).

168 To examine the role of DAN-c1 in aversive learning, we used a *Shibire*^{ts1} strain, which
169 encodes a thermosensitive mutant of dynamin blocking neurotransmitter release when the
170 ambient temperature is higher than 30°C by repressing endocytosis and vesicle recycling
171 functions[17]. When trained with QUI at 34°C, larvae with *Shibire*^{ts1} expression in DAN-c1 showed
172 significantly increased R.I. compared to that at room temperature (22°C), while it is not
173 significantly different from the DW at 34°C group (Figure 2f). The complete inactivation of
174 dopamine release from DAN-c1 with *Shibire*^{ts1} impaired aversive learning, indicating that
175 dopamine release from DAN-c1 is important for larval aversive learning to occur.

176 In the next experiments, a fly strain carrying temperature-sensitive cation channel, dTRPA1,
177 was used to excite the DAN-c1 neuron because it can be activated at temperatures higher than
178 30°C[57]. Compared to those at 22°C, activation of DAN-c1 with dTRPA1 at 34°C during training
179 induced repulsion to PA in the distilled water group, while it is not significantly different from the
180 QUI group at 22°C(Figure 2i). These data suggested that DAN-c1 excitation and presumably
181 increased dopamine release leads to larval aversive learning in the absence of gustatory pairing.

182 Combining the blockade results with *Shibire*^{ts1}, these data revealed that dopamine released
183 from DAN-c1 activation mediates larval aversive learning. However, when paired with a gustatory
184 stimulus (QUI or SUC), activation of DAN-c1 during training impairs both aversive and appetitive
185 learning (Figure 2i). We suggest that these data indicate a critical role for the amount of

186 dopamine release from DAN-c1 in larval associative learning, as dTRPA1 stimulation may result
187 in excessive dopamine release (see the **Discussion** section).
188
189 **The expression pattern of D2R in the third-instar larval brain.**
190 Although dopamine D1-like receptors have been proven important for learning[40], the role of
191 D2-like receptors has not been fully investigated. In addition, the expression pattern of D2R in fly
192 brains was not reported. A fly strain expressing GFP-tagged D2R (BDSC#60276) was used to reveal
193 the expression pattern of D2R in the third-instar larval brain (Figure 3a). D2Rs were found in
194 dopaminergic neurons and the mushroom body. In dopaminergic neurons (Figure 3b-g), D2Rs
195 were found in DM1, pPAM, DL2b, and some DL1 neurons. In the mushroom body, D2Rs were
196 expressed in the soma and lobes, but not in the calyx (Figure 3h and i). Even though D2Rs were
197 widely found in vertical lobes, medial lobes, and peduncles, they were not expressed in every
198 mushroom body neuron. A transection of the peduncle region showed the absence of D2Rs in
199 the core area (Figure S3i), which is composed of densely packed newly created fibers and lacks
200 Fasciclin II (FAS II)[47].
201 To inspect whether the pattern of GFP signals indeed reflected the expression of D2R, three
202 D2R enhancer driver strains (R72C04, R72C08, and R72D03-GAL4) were crossed with the GFP-
203 tagged D2R strain. R72C08-GAL4 covered three DM1 dopaminergic neurons (Figure S3c), and
204 R72C04-GAL4 labeled one DM1 and two DL2b dopaminergic neurons (Figure S3d and e). R72D03-
205 GAL4 identified parts of mushroom body neurons, whose axons spread on the surface of the
206 mushroom body lobes (Figure S3f); R72C08-GAL4 also identified a subset of neurons from four
207 MB neuroblasts, with soma in four clusters and a converged bundle of axons (Figure S3g and h).

208 These results revealed the expression of D2R in the mushroom body and dopaminergic neurons
209 in the third-instar larval brain.
210
211 **D2R in DAN-c1 influences larval aversive learning.**
212 Our previous work reported that D2R knockdown (UAS-RNAi) in dopaminergic neurons
213 driven by TH-GAL4 impaired larval aversive learning[62]. Using a microRNA strain (UAS-D2R-miR)[60],
214 a similar deficit was observed (Figure S4f). To further understand the roles of D2R in aversive
215 learning, its expression in distinct DANs, as well as corresponding learning assays were
216 investigated. Crossing the GFP-tagged D2R strain with a DAN-c1-mCherry strain demonstrated
217 the expression of D2R in DAN-c1 (Figure 4a).
218 To reduce the expression of D2R in dopaminergic neurons, a microRNA strain UAS-D2R-miR
219 was used when crossing with distinct driver strains. The efficiency of D2R knockdown was
220 confirmed by crossing the GFP-tagged D2R strain with TH-GAL4;UAS-D2R-miR. In these larval
221 brains, GFP signals in DM1 were not detected, while those in pPAM were still intact (Figure 4b
222 and c). Quantification showed a significant decrease of GFP signals in the knockdown group
223 compared to the control (Figure 4d), indicating reduced transcripts of D2R linked GFP by D2R-
224 microRNA (Figure S4c).
225 To investigate the roles of D2R in distinct dopaminergic neurons during larval associative
226 learning, UAS-D2R-miR strain was crossed with distinct driver strains labeling different pairs of
227 dopaminergic neurons. Among them, the knockdown of D2R in DAN-c1 impaired aversive
228 learning with the odorant pentyl acetate, while appetitive learning was unaffected (Figure 4e). In
229 contrast, although D2R was also found in DAN-d1 and DAN-g1, neither D2R knockdown in DAN-

230 d1 nor in DAN-g1 affected larval olfactory learning (Figure S4d-f, see the **Discussion** section). As
231 the naïve sensory and motor functions were not affected, this deficiency was caused by
232 impairment in learning abilities (Figure 4f-i). Similar learning deficits were observed in the same
233 strain trained with another odorant, propionic acid (Figure S5a), as well as in larvae with D2R
234 knockdown using UAS-RNAi (Figure S5b). These results demonstrated that D2Rs are expressed in
235 DAN-c1, and they are necessary for larval aversive learning. Presumably the knockdown of
236 presynaptic inhibitory D2R autoreceptors on DAN-c1 will result in increased and excessive
237 dopamine release, which leads to aversive learning deficiency. These results are consistent with
238 the activation studies with dTRPA1 above, in which increased dopamine release during training
239 results in impaired aversive learning (Figure 2i).
240
241 **Over-excitation of DAN-c1 during learning impairs larval aversive learning.**
242 To exclude possible chronic effects of D2R knockdown during development, optogenetics
243 was applied at distinct stages of the learning protocol. Channelrhodopsin2 (ChR2) is a blue light
244 activated cation channel from algae, which can be used to activate target neurons[63,64]. Over-
245 excitation of DANs under a TH-GAL4 driver with ChR2 during training impaired aversive learning
246 but left appetitive learning intact (Figure S7), which is consistent with D2R knockdown results. To
247 investigate the mechanisms with a better temporospatial resolution, ChR2 was expressed in
248 DAN-c1, and blue light was applied at distinct stages of the learning protocol (Figure 5a).
249 Optogenetic activation of DAN-c1 during training impaired aversive learning, not appetitive
250 learning (Figure 5b-d). This result is consistent with the effect of D2R knockdown in DAN-c1,

251 indicating that increased, excessive dopamine release during training leads to impaired aversive
252 learning.
253
254 **D2R in mushroom body mediates larval learning through inhibition.**
255 We have shown that D2R in DAN-c1 plays a critical role in larval aversive learning. Since D2Rs
256 are also expressed in soma and axons in most mushroom body neurons (Figure 3h and i), we
257 examined the role of D2R in MB neurons, a center for learning in *Drosophila*. Knockdown of these
258 D2Rs by D2R-miR impaired both appetitive and aversive learning (Figure 6a). Similarly,
259 optogenetic activation of mushroom body neurons during training led to deficiencies in both
260 appetitive and aversive learning (Figure 6b and d). These deficiencies were not observed in larvae
261 with activation during the resting stage. As D2Rs are inhibitory receptors, and optogenetic
262 activation leads to greater neuronal excitation like what may occur with knockdown of D2Rs,
263 these data show that the inhibitory effect of D2Rs in mushroom body neurons is necessary for
264 larval olfactory associative learning to occur.
265
266
267 **Discussion**
268 The dopaminergic system plays an important role in *Drosophila* olfactory associative
269 learning, but the roles of D2R in this process have not been fully explored. In this study, we
270 systematically investigated the expression pattern of D2R in the third-instar larval brain as well
271 as its role in larval aversive and appetitive learning. One driver strain identifying a pair of DAN-c1
272 neurons in the third-instar larval brain was discovered and learning assays with thermogenetic

273 tools (*Shibire*^{ts1}, dTRPA1) demonstrated that the blockade of dopamine release from DAN-c1
274 impeded aversive learning, while its activation during training led to repulsion toward the odor
275 in the absence of unconditioned stimulus (i.e., QUI). These results revealed that DAN-c1
276 activation (i.e., presumably leading to the release of synaptic dopamine) mediates larval aversive
277 learning to occur. Subsequently, the expression pattern of D2R was explored by using a GFP-
278 tagged D2R strain, including distinct dopaminergic and mushroom body neurons. D2Rs were
279 expressed in DAN-c1, and the knockdown of these receptors resulted in aversive learning
280 deficiency. These data suggested that presynaptic D2Rs in a pair of dopaminergic neurons, DAN-
281 c1, regulate dopamine release during excitation whereas knockdown of these same receptors
282 leads to excessive dopamine release, causing deficits in aversive learning to occur. Furthermore,
283 the activation of DAN-c1 with optogenetic tools during training, resulting in excessive dopamine
284 release, impaired aversive learning, as well. Finally, it was demonstrated that either the
285 knockdown of postsynaptic D2R or activation of mushroom body neurons led to learning deficits.
286 These data demonstrate that D2Rs in distinct brain locations are critically involved in associative
287 learning.
288
289 **The characteristics of the single odor larval learning paradigm**
290 We adopted the single odor larval learning paradigm from previous publications[17,18]. To
291 validate this paradigm induces associative learning responses, Honjo et al.[17,18] tested the
292 paradigm from four aspects: First, the paradigm did not show obvious sensitization or habituation
293 effects when larvae were tested. They applied the odorant to the larvae after training, only the
294 ones had paired training with both odor and unconditioned stimulus (quinine or sucrose) showed

295 learning responses. Larvae exposed for 30 minutes to either the odorant or the unconditioned
296 stimulus alone did not show a different response to the odor compared to the naïve group.
297 Second, the odor responses are associative. Honjo et al. showed only when the odorant was
298 paired with unconditioned stimulus would induce corresponding attraction or repulsion of larvae
299 to the odor. Neither odorant alone, unconditioned stimulus alone, nor temporal dissociation of
300 odorant and unconditioned stimulus would induce learning responses. Third, the odor responses
301 are odor specific. When applied to a second odorant that was not used for training, larvae only
302 showed learning responses to the odor paired with unconditioned stimulus. This result ruled out
303 the explanation of a general olfactory suppression and indicated larvae can discriminate and
304 specifically alter the responses to the odor paired with unconditioned stimulus. Although the
305 two-odor reciprocal training is not used, these results can show the association of unconditioned
306 stimulus and the corresponding paired odor. Finally, well known learning deficit mutants did not
307 show learned responses in this learning paradigm. Honjo et al. tested mutants (e.g., *rut* and *dnc*),
308 which showed learning deficits in the adult stage with two odor reciprocal learning paradigm[21,25].
309 These mutant larvae also failed to show learning responses when tested with the single odor
310 larval learning paradigm. Combining all the evidence above, we believe this single odor larval
311 learning paradigm is a robust and reliable paradigm for larval associative learning assays,
312 composing essential characteristics of classical conditioning. Previously, we applied this paradigm
313 to investigate the roles of mushroom body serotonin receptors (5-HT7) in larval appetitive
314 learning[65]. In this study, we used two distinct odorants (pentyl acetate and propionic acid), as
315 well as two D2R knockdown strains (UAS-miR and UAS-RNAi for D2R). We obtained similar results
316 for larvae with D2R knockdown in DAN-c1 using different odorants or D2R knockdown strains. In

317 addition, our naïve olfactory, naïve gustatory, and locomotion data ruled out the possibilities that
318 the responses were caused by impaired sensory or motor functions. Comparison with the control
319 group (odor paired with distilled water) ruled out the potential effects if habituation existed. All
320 these results support this single odor learning paradigm is reliable to assess the learning abilities
321 of *Drosophila* larvae. The failure of reduction in R.I. when larvae with D2R knockdown in DAN-c1
322 were trained in quinine paired with the odorant is caused by deficit in aversive learning ability.
323

324 **Insights into the neuronal circuits underlying larval olfactory associative learning.**

325 Mushroom body and dopaminergic neurons play important roles in *Drosophila* associative
326 learning in both larvae[66] and adults[66-69]. Combining our results with previous learning circuitry
327 research in adult flies and larvae, we hypothesized the mechanism underlying larval olfactory
328 associative learning. Olfactory information (odors, Conditioned Stimulus, CS) is received by
329 olfactory sensory neurons (OSN), then transmitted to the mushroom body via projection neurons
330 (PN)[70]. The mushroom body (MB) is a primary learning center of *Drosophila* and composed of
331 Kenyon cells (KC, or mushroom body neurons, MBN)[71-73]. Their dendrites form the calyx, receiving
332 olfactory information from projection neurons. The axons converge into peduncles, then branch
333 into the vertical and medial lobes. Distinct gustatory cues (taste, Unconditioned Stimuli, US) are
334 sensed by gustatory sensory neurons (GSN) and transferred to dopaminergic neurons in different
335 clusters (Figure 7a). DAN-c1 in the DL1 cluster mediates aversive cues, projects to the lower
336 peduncle (LP) in the mushroom body. The plasticity of synapses from MBNs to MB output
337 neurons (MBON) may be negatively modulated by dopamine, like those in adults[67,74,75]. The MBN-

338 MBON synapses in the vertical lobe and peduncle are responsible for attraction, while those in
339 the medial lobe are for repulsion.

340 When only the odorant appears, the subset of Kenyon cells representing this odor may be
341 depolarized, inducing calcium influx as in adult flies[73]. As a balance exists between compartments
342 across the mushroom body lobes, the response to the odor depends on the naïve olfactory
343 circuits from projection neurons to the lateral horn (LH). In aversive learning, in addition to
344 olfaction induced calcium influx, gustatory stimuli also lead to dopamine release from DAN-c1
345 and subsequently, activation of $G\alpha_s$ in LP. The co-existence of calcium and $G\alpha_s$ activates a Ca^{2+}-
346 dependent adenylate cyclase (AC), rutabaga (rut, as in adults[76-79]). Rutabaga converges
347 information from both olfaction and gustation, working as the coincidence detector of
348 associative learning. Its downstream signaling inhibits attractive MBN-MBON synapses in the LP,
349 breaking the balance between distinct compartments. As a result, after learning, the larvae will
350 exhibit repulsion when exposed to the odor again. In contrast, dopaminergic neurons in the
351 pPAM convey appetitive cues, which project to compartments in the medial lobe. The co-
352 existence of olfactory and appetitive gustatory stimuli leads to inhibition of these repulsive MBN-
353 MBON synapses, inducing attraction.

354

355 **The conserved role of DAN-c1 in aversive learning throughout *Drosophila* development.**

356 Adult *Drosophila* share similar neuronal circuits of learning with larvae[28,53,66-69]. In adult brains,
357 dopaminergic neurons are classified into 13 clusters, named as PAM (protocerebral anterior
358 medial), PAL (protocerebral anterior lateral), PPM (protocerebral posterior medial), PPL

359 (protocerebral lateral), and PPD (protocerebral posterior dorsal) clusters[80]. DANs in the PAM
360 cluster innervate the medial lobe, while those in PPL1 project to the vertical lobe[69].
361 R76F02-AD;R55C10-DBD identifies two dopaminergic neurons in adult brains, MB-MP1 in
362 PPL1 and ALT-PLPC in PPL2ab[60]. MB-MP1 is also named PPL1-γ1pedc, innervating both γ1 and the
363 peduncle of the β lobe[69]. Activation of this neuron induced aversive learning[61], and activation of
364 its corresponding MBON-γ1pedc>α/β led to approach[81]. During metamorphosis, dopaminergic
365 neurons in DL1 develop into the PPL1 cluster, DL2a neurons develop into PPL2ab, and those in
366 pPAM will develop into the PAM cluster[82]. This driver strain only identifies DAN-c1 from DL1 in
367 larvae, which innervates the lower peduncle of the mushroom body. Interestingly, previous
368 reports revealed that memory can be transferred from larvae to adults[83], indicating the
369 maintenance of neuronal circuitry architecture during metamorphosis. This evidence supports
370 that DAN-c1 is the corresponding neuron of PPL1-γ1pedc in larvae, which performs similar
371 functions in aversive learning.
372
373 **Pre- and post-synaptic D2Rs regulate cAMP in the mushroom body during aversive learning.**
374 The molecular mechanisms underlying *Drosophila* learning have not been fully determined.
375 In a traditional view, gustatory cues elevate dopamine release, which binds to D1 receptors and
376 then activates $G\alpha_s$. The co-existence of $G\alpha_s$ and calcium elicited by olfactory cues activates
377 rutabaga in axons of MBNs. Rutabaga transforms ATP into cAMP, activating PKA signaling
378 pathway. Mutant flies with either insufficient (*rutabaga*) or excessive cAMP (*dunce*) showed
379 aversive learning deficiency, indicating that the level of cAMP should be kept in an optimal range
380 to achieve aversive learning[21,25] (Figure 7b).

381 Our results have shown that D2Rs in dopaminergic neurons and the mushroom body are
382 important for larval aversive learning, suggesting a "*dual brake*" role in regulating cAMP levels in
383 the MBNs through both pre- and postsynaptic components. On the presynaptic side, D2R in DAN-
384 c1 decreases the release of dopamine under gustatory stimuli, reducing the probability of
385 postsynaptic D1R activation in MBNs. On the postsynaptic side, D2R in MBNs inhibits the
386 coincidence detector rutabaga (AC) both via activation of $G\alpha_{i/o}$ and inhibition of voltage-gated
387 calcium channels[2], indicating postsynaptic D2R functioning as a "*brake of the coincidence*
388 *detector"*. Combining these, "*dual brake*" D2R ultimately regulates the mushroom body cAMP
389 level within a physiologically optimal range during aversive learning. In addition, D2R fine tunes
390 the functional concentration spectrum of dopamine with higher resolutions, as its dopamine
391 affinity is 10- to 100-fold greater than D1 receptors. Overall, D2Rs work in a "*dual brake*" system
392 both expanding the representation of a dynamic range of gustatory signal intensity with high
393 signal to noise ratio and preventing postsynaptic overexcitation, which increases the reliability of
394 DAN-c1 and MBN circuits for the larval aversive learning (Figure 7c and d).

395 Recent studies showed that the approach/repulsion in adult learning is achieved via inhibition
396 of the repulsive/attractive representing compartments[67,74,75], which indicates dopamine inhibits
397 acetylcholine release from MBN to MBON[84]. However, the PKA signaling pathway usually
398 elevates neuronal excitability and increases neurotransmitter release[2,3], which is contradictory
399 to the recent findings[85]. In addition to the "*dual brake*" role of D2R, our results suggest a third
400 role of D2R in aversive learning. D1 and D2 receptors can form heteromeric receptors, whose
401 downstream $G\alpha_q$ activates PKC and CaMKII signaling pathways. The activation of these signaling
402 pathways may reduce acetylcholine release[86] (Figure 7c and d).

403

404 **Explanation of the results of thermogenetic and optogenetic experiments.**

405 Activation of DAN-c1 with dTRPA1 induced aversive learning, while the repulsion
406 disappeared when DAN-c1 was activated in the quinine group (Figure 2i). Our explanation is that
407 quinine stimulation and temperature activation led to over-excitation of DAN-c1, which impaired
408 aversive learning. This is consistent with the learning deficiency in larvae with D2R knockdown in
409 DAN-c1 (Figure 4e). Results from optogenetic activation of DAN-c1 during aversive learning also
410 support this (Figure 5b). However, in contrast to results with thermo-activation, larvae with
411 optogenetic activation of DAN-c1 showed neither repulsion after being trained with distilled
412 water (Figure 5c), nor did they show reduced attraction in the sucrose group (Figure 5d). One
413 possible explanation is that the thermo-activation is relatively mild compared to the optogenetic
414 activation. Based on this, thermo-activation of DAN-c1 is still in the physiological range of cAMP
415 under the upper limit (Figure 7b), resulting in repulsion in the distilled water (DW) group,
416 neutralized attraction in SUC group, and impaired repulsion in QUI group. In contrast,
417 optogenetic activation of DAN-c1 overwhelmed the physiological conditions, leading to failure of
418 repulsion in DW group (Figure 5c). This repulsive failure did not affect appetitive learning (Figure
419 5d), and a stronger over-excitation in QUI group induced similar failure (Figure 5b).

420

421 **Distinct dopaminergic neurons may have different roles in larval aversive learning.**

422 Although D2Rs are also expressed in DAN-d1 and DAN-g1 (Figure S4d and e), the knockdown
423 of D2R in these neurons did not impair larval aversive learning (Figure S4f). For DAN-g1,
424 interestingly, the R.I. from D2R knockdown larvae trained with quinine (QUI, aversive learning)

425 showed significant difference when compared to the DW (control) group, but it was also
426 significant different from the DAN-g1 genetic control group trained with QUI (two-way ANOVA,
427 Tukey's multiple comparisons, p=0.0002), while not significant different from UAS-D2R-miR
428 genetic control group trained with QUI (p=0.2724). Besides, D2R knockdown in DAN-g1 when
429 trained with another odorant propionic acid (ProA) did not show aversive learning deficiency
430 (Figure S5a). In addition, knockdown D2R in DAN-g1 using RNAi also did not show aversive
431 learning deficiency when trained with odorant pentyl acetate (PA, Figure S5b). This discrepancy
432 may be caused by the different stimulus intensity of distinct odorants, as well as the different
433 efficiency of distinct knockdown methods (microRNA or RNAi strains we used). We supposed that
434 D2Rs in DAN-g1 may partially affect larval aversive learning in a quantitative level; but not play
435 an important role as those in DAN-c1, which will cause a qualitative change when knockdown.

436 Previous work reported that aversive olfactory learning was induced through the optogenetic
437 activation of DAN- d1, f1, or g1, but not DAN-c1[87]. This discrepancy can be explained as the
438 optogenetic overexcitation of DAN-c1, similar to our optogenetic or D2R knockdown results. Our
439 learning assay results from larvae with D2R knockdown in DAN-d1 or g1 also supported this:
440 aversive learning was not affected by D2R knockdown (Figure S4f). These data indicate D2Rs in
441 DAN-d1 or g1 may not be important in larval aversive learning. Additionally, the DAN-c1 strain
442 used in the previous work (SS02160-split-GAL4) not only labels DAN-c1, but also marks other non-
443 dopaminergic neurons, which may affect the results. Besides, live calcium imaging showed that
444 DAN-d1, f1, and g1 responded to the activation of mechanosensory and nociceptive neurons[87],
445 indicating a functional differentiation from gustatory activated DAN-c1[61,88].

446 In future studies, the molecular signaling downstream of D2R needs to be explored, as well
447 as the comprehensive neuronal circuit architectures of larval learning. The neuronal circuits
448 underlying learning and memory are complex networks, sharing similarities with the regulatory
449 networks of gene expression. Studies of the mechanisms of learning and memory help us
450 understand the essential principles of the non-linear dynamic characteristics in these complex
451 systems. On one hand, the progress in larval learning provides useful information for helping our
452 understanding about more complex systems, from brains in adult flies to those in mammals. On
453 the other hand, the architecture of larval learning circuits could improve either hardware design
454 or algorithm structures in artificial intelligence, which may bring more powerful tools, such as
455 navigation systems regulating multiple auto-drive vehicles in complex 3-dimentional
456 environments.

457 In conclusion, we explored the expression pattern of D2R in the third-instar larval brain and
458 investigated their roles during larval olfactory learning. D2Rs were found in DAN-c1, and their
459 knockdown induced deficiency in aversive learning. D2Rs were also expressed in MBNs,
460 knockdown of which impaired both aversive and appetitive learning. This research revealed the
461 important roles of D2Rs in *Drosophila* larval olfactory learning and enriched our understanding
462 regarding the mechanisms underlying the learning process.

463 **Materials and Methods:**
464

465 ***Fly stocks*** All fly strains used in this study are listed in Table 1 and Table S1. Flies were maintained
466 on standard medium, which consists of cornmeal, yeast, dextrose, sucrose and agar in water.
467 Flies were kept in a 12/12-hour light/dark cycle at 25℃. Canton-S genotype (WT) and yw^{1118} were
468 used as wild-type. Strains carrying more than one transgene were constructed by standard
469 genetic crosses with the w^{1118}; CyO/Sco; TM2/TM6 multiple balancer chromosome strain. Strain
470 UAS-Syb::spGFP1-10, LexAop-CD4::GFP11, LexAop-rCD2::RFP /CyO; MB247-LexA::Up16/TM6B
471 was made by chromosome swapping between UAS-Syb::spGFP1-10, LexAop-CD4::GFP11/CyO (II,
472 second chromosome) and LexAop-rCD2::RFP (II).
473 The D2R gene is located on the X chromosome, with 6 different alternative splicing products.
474 The GFP-tagged D2R strain is inserted with a GFP gene in the second intron, generating D2R
475 molecules tagged with GFP[89,90]. The D2R-miR strain produces microRNA recognizing the
476 sequence across the third and fourth exons, which is not affected by the GFP insertion (Figure
477 S4c).
478 ***GRASP*** Split-GFP reconstitution across synaptic partners (GRASP) was used to investigate
479 whether neurons formed synapses[50] (Figure S2d). Half of split GFP tethered to the presynaptic
480 synaptobrevin (UAS-syb::spGFP1-10) was expressed in one type of neuron using UAS/Gal4 binary
481 system, and the complementary split GFP linked to a membrane protein (LexAop-CD4::spGFP11)
482 was expressed in another category of neuron with LexA/LexAop. If synapses between these
483 neurons exist, the split GFPs would form a complete one and be recognized by a mouse antibody
484 (Figure S2a-c).

485 ***Immunohistochemistry*** All staining processes were performed in 1.5 ml Eppendorf tubes. Late
486 third-instar (96-100h after egg laying) larval brains were dissected in dissection solution (300
487 mOsmol/L). Brains were fixed in 4% paraformaldehyde (PFA, Electron Microcopy Sciences, Cat.
488 No. 15713) for 1 hour on ice. After three washes (0.1% bovine serum albumin in 10mM PBS,
489 Sigma Life Sciences A9647), brains were incubated in the blocking and permeabilization solution
490 (0.2% Triton X-100 in 10mM PBS with 5% normal goat serum; Triton-X 100, Sigma, T8532; NGS,
491 Sigma-Aldrich, G9023) for 2 hours at room temperature. Incubation with primary antibodies was
492 done overnight at 4°C. After three washes, brains were incubated in the secondary antibodies
493 for two hours. Both the primary and secondary antibodies were diluted in the blocking and
494 permeabilization solution. GFP antibody (Rabbit, Thermo Fisher Scientific, Cat. No. A6455,
495 1:1000), TH antibody (Mouse, Immunostar, Cat. No. 22941, 1:1000), goat anti-rabbit with green
496 fluorescence (Invitrogen, Alexa Fluor 488 conjugate, Cat. No. A-11035, 1:1000), and goat anti-
497 mouse IgG with far-red fluorescence (Alexa Fluor 633 conjugate, Cat. No. 21052, 1:500)
498 secondary antibodies were used. After three washes, brains were transferred and mounted in
499 the Fluoro-Gel with Tris Buffer (Electron Microcopy Sciences, Cat. No. 17985-10) on a piece of
500 micro cover glasses (Electron Microcopy Sciences, Cat. No. 72200-41). Finally, the samples were
501 covered with another piece of micro cover glasses.

502 A seven-day staining protocol was used for staining GFP-tagged D2R or GRASP, in which
503 brains were fixed in 1% paraformaldehyde in Schneider's insect medium (Sigma Life Sciences,
504 Cat.NO. S0146) overnight at 4°C. In the second day, the brains were rinsed and washed twice
505 with PAT3 solution (0.5% Triton X-100 in 10mM PBS with 0.5% BSA), each for 1 hour. Then brains
506 were incubated in the blocking and permeabilization solution (3% NGS in PAT3) for 2 hours at

507 room temperature. Incubation of primary antibodies was done overnight at 4°C. On the third day,
508 brains were rinsed and washed twice with PBT solution, then incubated in the secondary
509 antibodies for five days. Both the primary and secondary antibodies were diluted in the PBTN
510 solution. In the staining of GFP-tagged D2R, GFP antibody (Rabbit, ThermoFisher Scientific, Cat.
511 No. A6455, 1: 1000), TH antibody (Mouse, Immunostar, Cat. No. 22941, 1:1000), and mCherry
512 antibody (Rat, ThermoFisher Scientific, Cat. No. M11217, 1:1000) were used. For staining of
513 GRASP, GFP antibody (Mouse, ThermoFisher Scientific, Cat. No. G6539, 1:100) was used. Goat
514 anti-rabbit with green fluorescence (Invitrogen, Alexa Fluor 488 conjugate, Cat. No. A-11035,
515 1:1000), goat anti-mouse with green fluorescence (Alexa Fluor 488 conjugate, Cat. No. A11029,
516 1:1000), goat anti-mouse with far-red fluorescence (Alexa Fluor 633 conjugate, Cat. No. A21052,
517 1:500), and goat anti-rat with red fluorescence (Alexa Fluor 546 conjugate, Cat. No. A-11081,
518 1:1000) secondary antibodies were used. In the seventh day, brains were rinsed and washed
519 twice with PBT solution, and then transferred and mounted in the Fluoro-Gel with Tris Buffer on
520 a piece of micro cover glasses. Finally, the samples were covered with another piece of micro
521 cover glasses.
522 ***Confocal imaging*** All images were obtained with a Zeiss Laser Scanning Microscope 510 (LSM510,
523 Carl Zeiss, Inc., USA). Under 40× and 100× objective magnifications, images were collapsed from
524 confocal stacks of 1.0 µm optical slices. Under 25× objective magnifications, images were
525 collapsed from confocal stacks of 2.0 µm optical slices. Under 10× objective magnifications,
526 images were collapsed from confocal stacks of 12.5 µm optical slices. ImageJ software was used
527 to remove other signals outside of the mushroom bodies, as the background noise in GRASP is
528 strong.

529 ***Larval olfactory learning assays*** All control strains used in learning assays were homozygous
530 except DAN-c1×WT, while all experimental groups (D2R knockdown, thermogenetics, and
531 optogenetics) used were heterozygous by crossing the corresponding control strains. The single
532 odor learning paradigm was slightly modified from previous publication[17,18]. In brief, 25 to 50
533 third-instar larvae (92–96 h after egg laying) were trained on a 2.5% agar plate (100 mm petri
534 dish) covered with 2 mL of 1 M sucrose solution (SUC, Sigma, Cat. No. S1888) or 0.1% quinine
535 hemisulfate solution (QUI, Sigma, Cat. No. 22640). Distilled water (DW) was used as a control. An
536 odorant pentyl acetate (PA, 10μL, Sigma-Aldrich, CAT. No. 109584) was placed on a small piece
537 of filter paper (0.25cm^2 square) inside the lid. After 30 minutes, larvae were rinsed and
538 transferred to the middle line of a new 2.5% agar plate. A small piece of filter paper (0.25cm^2
539 square) with 2.5μL pentyl acetate was placed on one side of the plate, while distilled water on
540 the other side. After 5 min, the numbers of larvae in the two semicircular areas were counted
541 and the response index (R.I.) was calculated with the following equation (Figure 2e):

542 $$\boldsymbol{R.I.} = \frac{\boldsymbol{\#\ of\ larvae\ on\ odorant\ side\ in\ dashline - \#\ of\ larvae\ on\ DW\ side\ in\ dashline}}{\boldsymbol{Total\ \#\ of\ larvae\ on\ two\ sides\ in\ dashlines}}$$

543 ***Naïve Olfactory Test*** Larvae were transferred into the midline of test plates. 2.5μL of odorant
544 were added on a piece of filter paper (0.25cm^2 square) on one side and distilled water on the
545 other side. The number of larvae in two semicircular areas were counted and the R.I. was
546 calculated after 5 min.

547 ***Naïve Gustatory Test*** A petri dish with a median separator was used. Both sides were filled with
548 1% agar, with 2 mL of distilled water on the control side, and with 1 M sucrose (SUC) solution, or
549 0.1% quinine hemisulfate (QUI) solution on the test side. Twenty larvae were put on each side

550 near the midline and allowed to move for 5 min. Gustatory R.I. was calculated using the larvae
551 numbers on two sides[91].
552 ***Larval locomotion assay*** Individual larvae were placed on the surface of a plate of 2.5% agar
553 mixed with 1mL India ink. They were allowed to acclimate for 1 min, and then a video was
554 recorded for 30 seconds using a Moticam3 digital camera (Motic) and Motic Images Plus 2.0
555 software. The video was analyzed by the MTrack2 plug-in (from
556 http://valelab.ucsf.edu/~nico/IJplugins/MTrack2.html) in ImageJ. The path was recorded; scores
557 were quantified as the length traveled per minute as previously described[92]. As the locomotion
558 speed of DAN-c1 homozygous was slow, DAN-c1 × WT was used as the control group.
559 ***Learning assays with thermogenetics*** In learning assays with thermogenetics, 25 to 50 third-
560 instar larvae (92–96 h after egg laying) were trained on a 2.5% agar plate (100mm petri dish)
561 covered with 2 mL of 1 M SUC or 0.1% QUI. DW was used as a control. An odorant PA was placed
562 on a small piece of filter paper (0.25cm^2 square) inside the lid. Training plates were put in a water
563 bath either under 22°C or 34°C. After 30 minutes, larvae were rinsed and transferred to the
564 testing plate. After 5 min, the response index (R.I.) was calculated.
565 ***Learning assays with optogenetics*** In learning assays with optogenetics, egg laying plates with
566 1mM ATR (all-trans retinal, Sigma, Cat. No. R2500) were used. All-trans retinal (ATR) is a
567 necessary light-isomerizable chromophore for ChR2, which is not synthesized by *Drosophila*.[93,94]
568 Around 50 third-instar larvae were trained in a 35mm petri dish with 2 mL of either 1 M SUC
569 or 0.1% QH solutions. DW was used as a control. During training, an odorant was placed on a
570 small piece of filter paper (0.25cm^2 square) inside the lid. To activate channelrhodopsin2, a LED
571 (Luxeon Rebel Color LEDs, 07040 PB000-D, wavelength 470 nm) with a power supply (GW Instek,

572 Laboratory DC power supply Model GPS-1830D) was used. The intensity of the blue light was 25
573 mW, measured by a laser power meter (Sanwa, LP1). After being trained for 30 minutes, larvae
574 were rinsed and transferred to the middle line of a 2.5% agar plate in 100 mm test plate. A small
575 piece of filter paper (0.25cm^2 square) with pentyl acetate was placed on one side of the plate,
576 while distilled water on the other side. Then the number of larvae in the two semicircular areas
577 were counted and the R.I. was calculated after 5 min.

578 ***Quantification of D2R knockdown*** Quantification of the fluorescent intensity of D2R knockdown
579 was performed as follows. TH signals were used to define dopaminergic neurons, and the mean
580 fluorescent intensity of GFP in each neuron was calculated with subtraction of the background.
581 The mean intensity of DM1 was divided by that of pPAM in each brain, and the value in the
582 knockdown group was subsequently normalized with the control group.

583 ***Statistical Analysis*** Information for statistical analysis is provided in figure legends. In brief, two-
584 way ANOVA and Tukey's multiple comparison test were used in Figure 2f-j, Figure 4e, Figure 5b-
585 d, Figure 6a-d, and Figure S7; unpaired t-test was used in Figure 4d; one-way ANOVA and Tukey
586 multiple's comparison test were used in Figure 4f-i; two-way ANOVA and Dunnett's multiple
587 comparison test were used in Figure S4f, and Figure S5a-b; one-way ANOVA and Dunnett's
588 multiple comparison test were used in Figure S6a-i.

589 **Author contributions**

590 **Qi. C.:** Conceptualization, Methodology, Formal analysis, Investigation, Writing – Original
591 Draft, Visualization, **Qian. C.:** Writing – Review & Editing, **Steijvers. E.:** Writing – Review & Editing
592 **Colvin. R.:** Writing – Review & Editing **Lee. D.:** Conceptualization, Writing – Review & Editing,
593 Supervision, Funding acquisition

594

595

596 **Acknowledgements**

597 This work was partially supported by an NIH grant (AG065925) and an International Collaboration
598 Grant from Korea Institute of Science & Technology (Brain Science Institute), Seoul, Korea. CQ
599 was a recipient of the SEA and GSR awards from Ohio University. We thank Dr. J Hirsh (University
600 of Virginia), Dr. M. Wu (Johns Hopkins University), Dr. M. Zlatic and Dr. C. Eschbach (HHMI Janelia
601 Research Campus), Dr. M. Gallio (Northwestern University), Dr. A. Kopin (Tufts-New England
602 Medical Center), Dr. S. Tanda (Ohio University), Dr. B. Condron (University of Virginia), Dr. T.
603 Kitamoto (University of Iowa) for their kind gift of fly strains.

604

605 **Data Availability:** Data will be made available on request.

606

607 **Declaration of Interest**

608 The authors declare no competing interests.

609

610 **Figure legends**
611
612
613 **Figure 1. Identification of driver strains for a pair of dopaminergic neurons in the *Drosophila***
614 **larval brain. (a)** A schematic diagram shows the dopaminergic neuron (DAN) clusters and the
615 mushroom body (MB) in the third-instar larval brain. **(b)** & **(c)** Schematic diagrams show the
616 innervation patterns from distinct DANs to different compartments in the MB. All 11 MB
617 compartments are shown, note that there is no synapse formed from dopaminergic neurons
618 (DANs) to the calyx and intermediate peduncle (IP). DANs in DL1 (b) and in pPAM (c). **(d-m)**
619 Drivers covering DANs in the DL1 cluster (d-h). Drivers covering DANs in the pPAM cluster (i-m).
620 The first column shows drivers covering distinct dopaminergic neurons. Neurons under the
621 drivers are labeled by GFP, the mushroom body (MB) is labeled by RFP, and DANs are marked by
622 tyrosine hydroxylase (TH) antibody. The second column (d'-m') shows the GRASP signals from
623 DANs under the driver to the corresponding compartments in the MB. The green channel
624 represents the GRASP signals, and RFP marks the morphology of the MB. In the first column,
625 white arrows mark the DANs under the driver strains. Yellow arrows in (d) show the pPAM
626 neurons not labelled by TH-GAL4 driver strain. The yellow arrowhead in (k) showed the DL1
627 neuron not innervating the MB. Scale bars: 50 µm for the first column, and 20 µm for the second
628 column. ***Abbreviations:*** DL, dorsolateral; DM, dorsomedial; IP, intermediate peduncle; IT
629 intermediate toe; IVL, intermediate vertical lobe; LA, lateral appendix; LP, lower peduncle; LT,
630 lower toe; LVL, lower vertical lobe; pPAM, primary protocerebral anterior medial; SHA, shaft; UT,
631 upper toe; UVL, upper vertical lobe. *(Note) GFP expression patterns in the entire larval CNS by*
632 *GAL4 driver strains used in this study can be found in Figure S1. N numbers for each strain can be*
633 *found in Table S2.*
634
635
636 **Figure 2. Dopamine release from DAN-c1 mediates larval aversive learning. (a-d)** R76F02-
637 AD;R55C10-DBD driver is used as it covers one dopaminergic neuron, DAN-c1, in each brain
638 hemisphere. **(a)** Dendrites and axons of DAN-c1 are labeled by DenMark and sytGFP,
639 correspondingly. **(b** and **c)** Soma and neurites from Figure 1f with higher magnification. DAN-c1
640 is labeled with GFP, the MB with RFP, and DANs with TH antibody (blue color). Only one DAN
641 soma is identified (b), axons from DAN-c1 innervate the lower peduncle (LP) of the MB (c). A
642 schematic diagram (**d**) shows the innervation patterns of DAN-c1. Modified from Eichler *et al.*[44],
643 and Saumweber *et. al*.[28]. **(e)** A schematic paradigm for larval olfactory learning (top) and two
644 different training paradigms for thermogenetics (bottom). **(f-h)** Blocking dopamine release from
645 DAN-c1 during learning using *shibire*^{ts1} strain at 34°C impairs larval aversive learning. **(h-j)**
646 Activation of DAN-c1 with dTRTPA1 at 34°C induces aversive learning. **QUI,** quinine. **DW,** distill
647 water. **SUC,** sucrose. Data are shown as mean ± SEM. Two-way ANOVA, Tukey's multiple
648 comparison test. For N numbers, interaction p-values, row factor p-values, and column factor p-
649 values, see Table S4. Scale bars: 50 µm (a), 20 µm (b and c). *(Note) N numbers of immunostaining*
650 *for each strain can be found in Table S2.*
651
652

653 **Figure 3. D2Rs are expressed in dopaminergic neurons and mushroom body in *Drosophila***
654 **larval brains. (a)** The expression pattern of D2R in a general view. D2R is shown with tagged GFP
655 (D2R-GFP). Magenta represents neuropils marked by nc82 antibody (a'). **(b-g)** D2Rs (presynaptic)
656 are found in most DANs: DM1a (**b**) and DM1b (**c**), pPAM (**d**), DL1 **(e)**, DL2a **(f)**, and DL2b **(g)** clusters.
657 D2Rs are expressed in parts of DL1 neurons (white arrows in **e**) but not in DL2a neurons (yellow
658 arrow heads in **f**). **(h-i)** D2Rs (postsynaptic) are found in soma of mushroom body (MB) neurons
659 (white arrows in **h**), and MB lobes and peduncles (**i**), but not in calyx (yellow arrow heads in **h**).
660 **(j)** A schematic diagram shows the expression pattern of pre- and postsynaptic D2R in DANs and
661 MB (yellow) in the *Drosophila* larval brain, respectively. Scale bars: 200 µm (a); 50 µm (b-g); 20
662 µm (h, i). ***Abbreviations:*** DL, dorsolateral; DM, dorsomedial; pPAM, primary protocerebral
663 anterior medial. *(Note) N numbers can be found in Table S2.*
664
665
666 **Figure 4. Presynaptic D2R in DAN-c1 is necessary for larval aversive learning. (a)** D2R is
667 expressed in DAN-c1. The expression pattern of D2R is shown with tagged GFP, DAN-c1 is marked
668 by mCherry, and all DANs are marked with TH antibody (blue). **(b-c)** Knockdown of D2R by D2R-
669 miR reduces fluorescent intensities of D2R-tagged GFP (D2R-GFP). The TH-GAL4 driver is used to
670 express mCherry. The intensity of D2R-tagged GFP is reduced in the DM1 cluster (yellow
671 arrowheads in b), which is still intact in pPAM neurons (white arrows in c). **(d)** D2R-GFP
672 fluorescent intensity is quantified by standardizing the values in DM1 with those in the pPAM.
673 Data are shown as mean ± SEM. For the TH-GAL4 group, N=7 brains; for the TH×D2R-miR group,
674 N=6 brains. Unpaired t-test, $p = 0.0125$. **(e)** Knockdown of D2R in DAN-c1 by D2R-miR impairs
675 larval aversive learning. **QUI,** quinine. **DW,** distill water. **SUC,** sucrose. Data are shown as mean ±
676 SEM. Two-way ANOVA, Tukey's multiple comparison test, $p < 0.0001$ for interaction, row factor
677 (genotype), and column factor (US) p-values. For N numbers, see Table S5. **(f-i)** D2R knockdown
678 in DAN-c1 does not affect naïve sensory and motor functions. Data are shown as mean ± SEM.
679 One-way ANOVA, Tukey's multiple comparison test. For N numbers, see Table S5. Scale bar: 20µm.
680 *(Note) Figures S5 and S6 show additional information on naïve sensory and motor functions in*
681 *larvae related to D2R-miR experiments. N numbers of immunostaining for each strain can be*
682 *found in Table S2.*
683
684
685 **Figure 5. Over-excitation of DAN-c1 impairs larval aversive learning. (a)** A schematic diagram
686 of optogenetic manipulations of neuronal excitability in DAN-c1 during distinct stages in learning.
687 **(b-d)** Activation of DAN-c1 during training impairs larval aversive learning (**b**), while keeps
688 appetitive learning intact (**d**). Unconditioned stimuli used were quinine (b) and sucrose (d). No
689 learning behaviors are observed in the control distilled water (DW) groups (**c**). Third-instar larvae
690 with ChR2 expression in DAN-c1 are used. *ATR,* all-trans-retinal. Data are shown as mean ± SEM.
691 Two-way ANOVA, Tukey's multiple comparison test. In QUI group p-values (b), $p = 0.0009$ for
692 interaction, $p < 0.0001$ for row factor (training stages), and $p = 0.1365$ for column factor (whether
693 with ATR); in DW group p-values (c), $p = 0.8367$ for interaction, $p = 0.9750$ for row factor (training
694 stages), and $p = 0.4872$ for column factor (whether with ATR); in SUC group p-values (d), $p =$
695 0.6247 for interaction, $p = 0.2550$ for row factor (training stages), and $p = 0.9437$ for column
696 factor (whether with ATR). For N numbers, see Table S6.

697
698 **Figure 6. D2R in mushroom body is necessary for both aversive and appetitive learning. (a)**
699 Knockdown D2R in mushroom body neurons (MBNs) impairs larval aversive and appetitive
700 learning. **(b-d)** Activation of MBNs during training impairs both larval aversive and appetitive
701 learning. Unconditioned stimuli used were quinine (b) and sucrose (d). No learning behaviors are
702 observed in the control distilled water (DW) groups (c). Third-instar larvae with ChR2 expression
703 in MBNs (201Y-GAL4) are used. *ATR,* all-trans-retinal. Data are shown as mean ± SEM. Two-way
704 ANOVA, Tukey's multiple comparison test. In D2R knockdown experiments (a), $p < 0.0001$ for
705 interaction, $p = 0.0011$ for row factor (genotype), and $p < 0.0001$ for column factor (US). In
706 optogenetic QUI group (b), $p = 0.0259$ for interaction, $p < 0.0001$ for row factor (training stages),
707 and $p = 0.0040$ for column factor (whether with ATR); in DW group (c), $p = 0.8077$ for interaction,
708 $p = 0.7623$ for row factor (training stages), and $p = 0.5846$ for column factor (whether with ATR);
709 in SUC group p-values(d), $p = 0.0035$ for interaction, $p = 0.0086$ for row factor (training stages),
710 and $p = 0.0865$ for column factor (whether with ATR). For N numbers, see Table S5 and S6.
711
712
713 **Figure 7. Roles of D2Rs in dopaminergic and mushroom body neurons during larval**
714 **olfactory learning. (a)** A schematic diagram shows the roles of D2R in dopaminergic neurons
715 (DAN) and mushroom body neurons (MBN) in larval olfactory associative learning**.** During
716 learning, olfactory stimuli (conditioned stimulus, CS) are received by olfactory sensory neurons
717 (OSN) and transmitted to MBNs (green) via projection neurons (PN). Distinct gustatory stimuli
718 (unconditioned stimulus, US) are received by gustatory sensory neurons (GSN) and transferred
719 to different dopaminergic neurons. Aversive stimuli are sent to DAN-c1 (red) in the DL1 cluster
720 which connects the lower peduncle compartment (LP, square in dash line), while appetitive
721 stimuli are received by pPAM neurons (blue) innervating the medial lobe (ML). D2Rs (yellow
722 square) are expressed in DAN-c1 and pPAM as autoreceptors, regulating dopamine release. Both
723 D2R and dDA1 (magenta circle) are expressed in the MBNs. **(b)** A hypothetical curve showing the
724 relationship between learning ability and cAMP level in the mushroom body. Insufficient cAMP
725 (*rutabaga mutant*) cannot induce learning, while excessive cAMP (*dunce mutant*) also impairs
726 learning. Only the appropriate level of cAMP regulated by the opposing actions of D1R (dDA1)
727 and D2R leads to successful learning in wild type larvae (WT). Knockdown of D2R in DAN-c1
728 causes excessive dopamine release, elevating cAMP and resulting in impaired learning. D2R
729 knockdown in MBNs relieves the inhibition effect of D2R, resulting in excessive intracellular cAMP
730 and learning failure. **(c-d)** Potential molecular mechanisms underlying *Drosophila* olfactory
731 learning in the square region shown in (a). **(d)** During aversive learning, olfactory stimuli induce
732 depolarization of MBNs, which activates voltage-gated calcium channels and induces calcium
733 influx. Gustatory stimuli, such as quinine, activates dopaminergic neurons and elevates dopamine
734 (DA) release. D1 receptor (dDA1) activates adenylyl cyclase (AC) and elevates cAMP via $G\alpha_s$, while
735 D2 receptor (D2R) inhibits AC and suppresses cAMP via $G\alpha_{i/o}$. In *Drosophila*, the coincidence
736 detector *rutabaga* (AC) is activated by the existence of both calcium and $G\alpha_s$, converging the
737 olfactory and gustatory stimuli. cAMP activates the PKA signaling pathway, elevating the
738 neuronal excitability. D1 and D2 receptors can also form heteromeric receptors and activate the
739 PLC-PKC and CaMKII signaling pathways via $G\alpha_q$. These pathways inhibit acetylcholine (ACh)
740 release from MBNs to MB output neurons (MBON), which leads to avoidance of the learned odor.

741 ***Abbreviations:*** AC, adenylyl cyclase; ACh, acetylcholine; ATP, adenosine triphosphate; CaM,
742 calmodulin; CaMKII, Ca^{2+}/calmodulin-dependent protein kinase II; cAMP, cyclic adenosine
743 monophosphate; CS, conditioned stimulus; DA, dopamine; DAN, dopaminergic neurons; DL,
744 dorsolateral; ER, endoplasmic reticulum; $G\alpha_{i/o}$, $G_{i/o}$ protein α subunit; $G\alpha_q$, G_q protein α subunit;
745 $G\alpha_s$, G_s protein α subunit; GSN, gustatory sensory neurons; LP, lower peduncle; MBN, mushroom
746 body neurons; MBON, mushroom body output neurons; ML, medial lobe; nAChR, nicotinic
747 acetylcholine receptor; OSN, olfactory sensory neurons; PKA, protein kinase A; PKC, protein
748 kinase C; PLC, phospholipase C; PN, projection neurons; pPAM, primary protocerebral anterior
749 medial; RyR, ryanodine receptor; US, unconditioned stimulus; VGCC, voltage gated calcium
750 channel.
751
752
753 **Table 1. Driver strains screened for dopaminergic neurons in the third-instar larval brain.**
754 Strains are listed with their published names and names used in this work. The numbers of
755 dopaminergic and non-dopaminergic neurons in the third-instar larval brain are described. The
756 identities of dopaminergic neurons from distinct clusters are also listed, especially for those in
757 DL1 and pPAM. The analogs column lists the labelled neurons in previous publications.
758 Source/Gift column shows the original papers in which these strains were described, as well as
759 the laboratories these strains were obtained from. Several, 2-5 neurons; some, 6-10 neurons;
760 lots, >10 neurons
761

762 **Supplemental information**
763
764 **Figure S1. GFP expression patterns in the larval CNS by GAL4 driver strains used in this study.**
765 **(a-n)** Representative pictures show the patterns of distinct GAL4 driver strains crossed with a
766 UAS-GFP strain. **(o)** A representative picture shows the pattern of MB247-LexA driver (MB247-
767 LexA::VP16) crossed with a LexAop-RFP strain (LexAop-rCD2::RFP). Blue channel represents
768 neuropils marked by nc82 antibody. Driver strains in **(a-j)** were used in **Figure 1d-m.** Driver strains
769 in **(k-m)** are strains used in supplementary **Figure S3**. 201Y-Gal4 (**n**) is the driver strain used in
770 **Figure 6**. Square region is enlarged in **(p)** to show the soma and neurites. White arrows label the
771 soma of DAN-c1, while yellow arrow heads label other neurons. Summary of analysis can be
772 found in Table S3. Scale bar: 200 µm. ***(Note)*** *N numbers can be found in Table S2. In Figure 1 and*
773 *S1, we mainly showed the strains labeling distinct pairs of dopaminergic neurons. The labeling*
774 *patterns of the rest 47 strains screened were summarized in Table 1, whose brain images are*
775 *available and can be provided upon request.*
776
777
778 **Figure S2. Controls for GRASP experiments. (a-c)** The GRASP signals were not observed in
779 control groups. The first column shows the mouse anti-GFP staining (green) for GRASP signals,
780 the second column shows MB lobes by RFP (red), and the third column shows the rabbit anti-GFP
781 staining (blue) which only recognizes the spGFP1-10. **(a)** Both GRASP (mouse antibody, green)
782 and spGFP1-10 (rabbit antibody, blue) can be recognized in the lower peduncle (LP) compartment
783 (white arrows), in a larval brain expressing spGFP1-10 under TH-Gal4 and spGFP11 under MB247-
784 LexA. Some strong spGFP1-10 signals outside of MB are also colocalized with GRASP signals
785 (yellow arrowheads). **(b)** GRASP signals are hardly observed in a larval brain only expressing
786 spGFP1-10 under TH-Gal4 (no MB247-LexA in this brain), while anti-spGFP1-10 signals are still
787 strong (magenta arrows). **(c)** Neither GRASP nor spGFP1-10 can be recognized in a larval brain
788 only expressing spGFP11 under MB247-LexA (cyan arrowheads). Scale bars: 20 µm. **(d)** A
789 Schematic diagram shows the mechanism of GRASP. Modified from Macpherson et. al.[50]. *(Note)*
790 *N numbers can be found in Table S2.*
791
792
793 **Figure S3. D2R-GAL4 strains support the expression pattern of D2R. (a-b)** Control staining
794 for D2R-tagged GFP in Figure 3. The green channel represents GFP signals whereas magenta
795 represents neuropils marked by nc82 antibody. GFP staining in WT (a). Secondary antibody only
796 staining for the D2R-tagged GFP strain (b). **(c-e)** D2R-GAL4 strains support the expression of D2R
797 in some DANs. The green channel represents GFP signals, red represents mCherry signals under
798 D2R-GAL4 drivers, and blue marks DANs with TH antibodies. R72C08 labels three DM1 neurons
799 (c). R72C04 labels one DM1 (d) and two DL2b neurons (e). **(f-h)** D2R-GAL4 strains support the
800 expression of D2R in mushroom body neurons. The green channel represents GFP signals, and
801 red represents mCherry signals under D2R-GAL4 drivers. R72D03 marks some MBNs in
802 mushroom body (f). R72C08 labels some MBNs in axons (g), dendrites and soma (h). **(i)** D2R is
803 absent in the core of mushroom body lobes, from a transection view of the lower peduncle. Scale
804 bars: 200 µm (a and b); 20 µm (c-e, g-i), 50 µm (f). *(Note) N numbers can be found in Table S2.*
805

806
807 **Figure S4. D2Rs in DAN-d1 and DAN-g1 are not necessary for aversive learning. (a-b)**
808 Dendrites and axons of DAN-d1 (a) and g1 (b) are labeled by DenMark (red) and sytGFP (green),
809 correspondingly. **(c)** The gene structure of D2R, the insertion site of GFP, and the D2R-microRNA
810 targeting sequence are shown in a schematic diagram. Modified from Xie and Ho[60]. **(d-e)** D2Rs
811 are expressed in DAN-d1 (d) and DAN-g1 (e). The expression pattern of D2R is shown with tagged-
812 GFP, DAN-g1 and d1 are marked by mCherry, and DANs are labeled by TH-antibody (blue). **(f)**
813 Knockdown D2R in neither in DAN-g1 nor DAN-d1 impairs aversive learning. Data are shown as
814 mean ± SEM. UAS-D2R-miR data is from Figure 4e. Two-way ANOVA, Dunnett's multiple
815 comparison test. $p = 0.0544$ for interaction, $p < 0.0001$ for row factor (genotype), and $p < 0.0001$
816 for column factor (US). For N numbers, see Table S5. Scale bars: 50 µm (a and b), 20 µm (d and
817 e). *(Note) N numbers of immunostaining for each strain can be found in Table S2.*
818
819
820 **Figure S5. Knockdown D2R in DAN-c1 with a RNAi strain also impairs aversive learning. (a)**
821 Knockdown of D2R with D2R-miR in DAN-c1 impairs larval aversive learning when using propionic
822 acid as the odorant. **(b)** Knockdown of D2R in DAN-c1 with a RNAi strain also impairs larval
823 aversive learning when using pentyl acetate as the odorant, while knockdown of D2R in either
824 DAN-d1 or g1 does not affect learning. Data are shown as mean ± SEM. Two-way ANOVA,
825 Dunnett's multiple comparison test. In D2R-miR experiments (a), $p = 0.0009$ for interaction, $p <$
826 0.0001 for row factor (genotype), and $p < 0.0001$ for column factor (US); in D2R-RNAi experiments
827 (b), $p = 0.3802$ for interaction, $p = 0.0001$ for row factor (genotype), and $p < 0.0001$ for column
828 factor (US). For N numbers, see Table S5.
829
830
831 **Figure S6. Naïve sensory and motor functions of *Drosophila* larvae. (a-e)** The naïve sensory
832 and motor functions in larvae related to D2R-miR experiments. **(a)** No significant difference exists
833 between strains in naïve olfactory tests toward pentyl acetate (PA). **(b)** No significant difference
834 exists between strains in naïve olfactory tests toward propionic acid (ProA). **(c)** No significant
835 difference exists between strains in naïve gustatory tests toward quinine (QUI). **(d)** No significant
836 difference exists between strains in naïve gustatory tests toward sucrose (SUC). **(e)** No significant
837 difference is found between strains and WT, except DAN-c1. So, larvae from DAN-c1 × WT are
838 used for all behavioral assays (refer to **i**). **(f-i)** The naïve sensory and motor functions in larvae
839 related to RNAi experiments. **(f)** No significant difference exists between strains and WT. **(g)** No
840 significant difference exists between strains in naïve gustatory tests toward QUI. **(h)** No
841 significant difference exists between strains in naïve gustatory tests toward SUC. **(i)** There is a
842 significant difference between strains in larval locomotion speed, and there is significant
843 difference between DAN-d1, DAN-d1 × RNAi and WT, but these differences do not affect the
844 learning ability of larvae. Data are shown as mean ± SEM. One-way ANOVA, Dunnett's multiple
845 comparison test. For N numbers, see Table S5.
846
847
848 **Figure S7. Over-excitation of DANs during learning impairs larval aversive learning.** Third-
849 instar larvae with ChR2 expression in most DANs (TH-Gal4) were used. Activation of DANs during

training impairs larval aversive learning (**a**), while keeping appetitive learning intact (**c**). No learning behaviors are observed in the control distilled water (DW) groups **(b)**. Data are shown as mean ± SEM. Two-way ANOVA, Tukey's multiple comparison test. In QUI group (a), $p = 0.0011$ for interaction, $p = 0.0023$ for row factor (training stages), and $p < 0.0001$ for column factor (whether with ATR); in DW group (b), $p = 0.6126$ for interaction, $p = 0.0850$ for row factor (training stages), and $p = 0.5748$ for column factor (whether with ATR); in SUC group (c), $p = 0.8910$ for interaction, $p = 0.9239$ for row factor (training stages), and $p = 0.9503$ for column factor (whether with ATR). For N numbers, see Table S6.

Supplementary Tables

Table S1. Other strains used in this study.

Table S2. N numbers for brain samples used in Figures.

Table S3. Summary of R76F02AD;R55C10DBD (DAN-c1) identifying patterns in larval brains. For the strain R76F02AD; R55C10DBD, 22 third-instar larval brains expressing GFP or SytGFP and DenMark were examined, and all of them clearly identified DAN-c1. Half of them only identified DAN-c1, the rest had 1 to 5 weak identified cells without neurites, and barely 1 or 2 strong identified cells appeared. These non-DAN-c1 neurons were seldom dopaminergic neurons. In ventral nerve cord (VNC), 8 out of 12 did not have any identified cells, 3 had 2-4 strong identified cells. These data supported that R76F02AD;R55C10DBD exclusively labels DAN-c1 in third-instar larval brains.

Table S4. N numbers and p-values for learning assays with thermogenetics.

Table S5. N numbers for D2R knockdown experiments.

Table S6. N numbers for learning assays with optogenetics

881 **Reference:**

882 1 Kandel, E. R., Dudai, Y. & Mayford, M. R. The molecular and systems biology of memory.
883 *Cell* **157**, 163-186 (2014). https://doi.org/10.1016/j.cell.2014.03.001
884 2 Neve, K. A., Seamans, J. K. & Trantham-Davidson, H. Dopamine receptor signaling. *J*
885 *Recept Signal Transduct Res* **24**, 165-205 (2004). https://doi.org/10.1081/rrs-200029981
886 3 Baik, J. H. Dopamine signaling in reward-related behaviors. *Front Neural Circuits* **7**, 152
887 (2013). https://doi.org/10.3389/fncir.2013.00152
888 4 Missale, C., Nash, S. R., Robinson, S. W., Jaber, M. & Caron, M. G. Dopamine receptors:
889 from structure to function. *Physiol Rev* **78**, 189-225 (1998).
890 https://doi.org/10.1152/physrev.1998.78.1.189
891 5 Bjorklund, A. & Dunnett, S. B. Dopamine neuron systems in the brain: an update. *Trends*
892 *Neurosci* **30**, 194-202 (2007). https://doi.org/10.1016/j.tins.2007.03.006
893 6 Puig, M. V., Antzoulatos, E. G. & Miller, E. K. Prefrontal dopamine in associative learning
894 and memory. *Neuroscience* **282**, 217-229 (2014).
895 https://doi.org/10.1016/j.neuroscience.2014.09.026
896 7 Barrot, M. The ventral tegmentum and dopamine: A new wave of diversity.
897 *Neuroscience* **282**, 243-247 (2014). https://doi.org/10.1016/j.neuroscience.2014.10.017
898 8 Savica, R. & Benarroch, E. E. Dopamine receptor signaling in the forebrain: recent
899 insights and clinical implications. *Neurology* **83**, 758-767 (2014).
900 https://doi.org/10.1212/WNL.0000000000000719
901 9 Beaulieu, J. M. & Gainetdinov, R. R. The physiology, signaling, and pharmacology of
902 dopamine receptors. *Pharmacol Rev* **63**, 182-217 (2011).
903 https://doi.org/10.1124/pr.110.002642
904 10 Klein, M. O. *et al.* Dopamine: Functions, Signaling, and Association with Neurological
905 Diseases. *Cell Mol Neurobiol* **39**, 31-59 (2019). https://doi.org/10.1007/s10571-018-
906 0632-3
907 11 Waddell, S. Dopamine reveals neural circuit mechanisms of fly memory. *Trends Neurosci*
908 **33**, 457-464 (2010). https://doi.org/10.1016/j.tins.2010.07.001
909 12 Berry, J., Krause, W. C. & Davis, R. L. Olfactory memory traces in Drosophila. *Prog Brain*
910 *Res* **169**, 293-304 (2008). https://doi.org/10.1016/S0079-6123(07)00018-0
911 13 Bellen, H. J., Tong, C. & Tsuda, H. 100 years of Drosophila research and its impact on
912 vertebrate neuroscience: a history lesson for the future. *Nat Rev Neurosci* **11**, 514-522
913 (2010). https://doi.org/10.1038/nrn2839
914 14 Yamamoto, S. & Seto, E. S. Dopamine dynamics and signaling in Drosophila: an overview
915 of genes, drugs and behavioral paradigms. *Exp Anim* **63**, 107-119 (2014).
916 https://doi.org/10.1538/expanim.63.107
917 15 Heisenberg, M. Mushroom body memoir: from maps to models. *Nat Rev Neurosci* **4**,
918 266-275 (2003). https://doi.org/10.1038/nrn1074
919 16 Davis, R. L. Olfactory learning. *Neuron* **44**, 31-48 (2004).
920 https://doi.org/10.1016/j.neuron.2004.09.008
921 17 Honjo, K. & Furukubo-Tokunaga, K. Induction of cAMP response element-binding
922 protein-dependent medium-term memory by appetitive gustatory reinforcement in
923 Drosophila larvae. *J Neurosci* **25**, 7905-7913 (2005).
924 https://doi.org/10.1523/JNEUROSCI.2135-05.2005

18 Honjo, K. & Furukubo-Tokunaga, K. Distinctive neuronal networks and biochemical pathways for appetitive and aversive memory in Drosophila larvae. *J Neurosci* **29**, 852-862 (2009). https://doi.org/10.1523/JNEUROSCI.1315-08.2009

19 Widmann, A. *et al.* Genetic Dissection of Aversive Associative Olfactory Learning and Memory in Drosophila Larvae. *PLoS Genet* **12**, e1006378 (2016). https://doi.org/10.1371/journal.pgen.1006378

20 Quinn, W. G., Harris, W. A. & Benzer, S. Conditioned behavior in Drosophila melanogaster. *Proc Natl Acad Sci U S A* **71**, 708-712 (1974). https://doi.org/10.1073/pnas.71.3.708

21 Tempel, B. L., Bonini, N., Dawson, D. R. & Quinn, W. G. Reward learning in normal and mutant Drosophila. *Proc Natl Acad Sci U S A* **80**, 1482-1486 (1983). https://doi.org/10.1073/pnas.80.5.1482

22 Roman, G. & Davis, R. L. Molecular biology and anatomy of Drosophila olfactory associative learning. *Bioessays* **23**, 571-581 (2001). https://doi.org/10.1002/bies.1083

23 Quinn, W. G. & Dudai, Y. Memory phases in Drosophila. *Nature* **262**, 576-577 (1976). https://doi.org/10.1038/262576a0

24 Waddell, S., Armstrong, J. D., Kitamoto, T., Kaiser, K. & Quinn, W. G. The amnesiac gene product is expressed in two neurons in the Drosophila brain that are critical for memory. *Cell* **103**, 805-813 (2000). https://doi.org/10.1016/s0092-8674(00)00183-5

25 Dudai, Y., Jan, Y. N., Byers, D., Quinn, W. G. & Benzer, S. dunce, a mutant of Drosophila deficient in learning. *Proc Natl Acad Sci U S A* **73**, 1684-1688 (1976). https://doi.org/10.1073/pnas.73.5.1684

26 Davis, R. L. & Dauwalder, B. The Drosophila dunce locus: learning and memory genes in the fly. *Trends Genet* **7**, 224-229 (1991). https://doi.org/10.1016/0168-9525(91)90369-2

27 Crittenden, J. R., Skoulakis, E. M., Han, K. A., Kalderon, D. & Davis, R. L. Tripartite mushroom body architecture revealed by antigenic markers. *Learn Mem* **5**, 38-51 (1998).

28 Saumweber, T. *et al.* Functional architecture of reward learning in mushroom body extrinsic neurons of larval Drosophila. *Nat Commun* **9**, 1104 (2018). https://doi.org/10.1038/s41467-018-03130-1

29 Stocker, R. F. Drosophila as a focus in olfactory research: mapping of olfactory sensilla by fine structure, odor specificity, odorant receptor expression, and central connectivity. *Microsc Res Tech* **55**, 284-296 (2001). https://doi.org/10.1002/jemt.1178

30 Ramaekers, A. *et al.* Glomerular maps without cellular redundancy at successive levels of the Drosophila larval olfactory circuit. *Curr Biol* **15**, 982-992 (2005). https://doi.org/10.1016/j.cub.2005.04.032

31 Lee, T., Lee, A. & Luo, L. Development of the Drosophila mushroom bodies: sequential generation of three distinct types of neurons from a neuroblast. *Development* **126**, 4065-4076 (1999). https://doi.org/10.1242/dev.126.18.4065

32 Blanco, J., Pandey, R., Wasser, M. & Udolph, G. Orthodenticle is necessary for survival of a cluster of clonally related dopaminergic neurons in the Drosophila larval and adult brain. *Neural Dev* **6**, 34 (2011). https://doi.org/10.1186/1749-8104-6-34

967 33 Schroll, C. *et al.* Light-induced activation of distinct modulatory neurons triggers
968 appetitive or aversive learning in Drosophila larvae. *Curr Biol* **16**, 1741-1747 (2006).
969 https://doi.org/10.1016/j.cub.2006.07.023
970 34 Sugamori, K. S., Demchyshyn, L. L., McConkey, F., Forte, M. A. & Niznik, H. B. A
971 primordial dopamine D1-like adenylyl cyclase-linked receptor from Drosophila
972 melanogaster displaying poor affinity for benzazepines. *FEBS Lett* **362**, 131-138 (1995).
973 https://doi.org/10.1016/0014-5793(95)00224-w
974 35 Han, K. A., Millar, N. S., Grotewiel, M. S. & Davis, R. L. DAMB, a novel dopamine receptor
975 expressed specifically in Drosophila mushroom bodies. *Neuron* **16**, 1127-1135 (1996).
976 https://doi.org/10.1016/s0896-6273(00)80139-7
977 36 Hearn, M. G. *et al.* A Drosophila dopamine 2-like receptor: Molecular characterization
978 and identification of multiple alternatively spliced variants. *Proc Natl Acad Sci U S A* **99**,
979 14554-14559 (2002). https://doi.org/10.1073/pnas.202498299
980 37 Srivastava, D. P. *et al.* Rapid, nongenomic responses to ecdysteroids and catecholamines
981 mediated by a novel Drosophila G-protein-coupled receptor. *J Neurosci* **25**, 6145-6155
982 (2005). https://doi.org/10.1523/JNEUROSCI.1005-05.2005
983 38 Kim, Y. C., Lee, H. G., Seong, C. S. & Han, K. A. Expression of a D1 dopamine receptor
984 dDA1/DmDOP1 in the central nervous system of Drosophila melanogaster. *Gene Expr*
985 *Patterns* **3**, 237-245 (2003). https://doi.org/10.1016/s1567-133x(02)00098-4
986 39 Selcho, M., Pauls, D., Han, K. A., Stocker, R. F. & Thum, A. S. The role of dopamine in
987 Drosophila larval classical olfactory conditioning. *PLoS One* **4**, e5897 (2009).
988 https://doi.org/10.1371/journal.pone.0005897
989 40 Kim, Y. C., Lee, H. G. & Han, K. A. D1 dopamine receptor dDA1 is required in the
990 mushroom body neurons for aversive and appetitive learning in Drosophila. *J Neurosci*
991 **27**, 7640-7647 (2007). https://doi.org/10.1523/JNEUROSCI.1167-07.2007
992 41 Scholz-Kornehl, S. & Schwarzel, M. Circuit Analysis of a Drosophila Dopamine Type 2
993 Receptor That Supports Anesthesia-Resistant Memory. *J Neurosci* **36**, 7936-7945 (2016).
994 https://doi.org/10.1523/JNEUROSCI.4475-15.2016
995 42 Zhou, M. *et al.* Suppression of GABAergic neurons through D2-like receptor secures
996 efficient conditioning in Drosophila aversive olfactory learning. *Proc Natl Acad Sci U S A*
997 **116**, 5118-5125 (2019). https://doi.org/10.1073/pnas.1812342116
998 43 Draper, I., Kurshan, P. T., McBride, E., Jackson, F. R. & Kopin, A. S. Locomotor activity is
999 regulated by D2-like receptors in Drosophila: an anatomic and functional analysis. *Dev*
1000 *Neurobiol* **67**, 378-393 (2007). https://doi.org/10.1002/dneu.20355
1001 44 Eichler, K. *et al.* The complete connectome of a learning and memory centre in an insect
1002 brain. *Nature* **548**, 175-182 (2017). https://doi.org/10.1038/nature23455
1003 45 Tanaka, N. K., Tanimoto, H. & Ito, K. Neuronal assemblies of the Drosophila mushroom
1004 body. *J Comp Neurol* **508**, 711-755 (2008). https://doi.org/10.1002/cne.21692
1005 46 Kunz, T., Kraft, K. F., Technau, G. M. & Urbach, R. Origin of Drosophila mushroom body
1006 neuroblasts and generation of divergent embryonic lineages. *Development* **139**, 2510-
1007 2522 (2012). https://doi.org/10.1242/dev.077883
1008 47 Kurusu, M. *et al.* Embryonic and larval development of the Drosophila mushroom
1009 bodies: concentric layer subdivisions and the role of fasciclin II. *Development* **129**, 409-
1010 419 (2002). https://doi.org/10.1242/dev.129.2.409

1011 48 Rohwedder, A. *et al.* Four Individually Identified Paired Dopamine Neurons Signal
1012 Reward in Larval Drosophila. *Curr Biol* **26**, 661-669 (2016).
1013 https://doi.org/10.1016/j.cub.2016.01.012
1014 49 Friggi-Grelin, F. *et al.* Targeted gene expression in Drosophila dopaminergic cells using
1015 regulatory sequences from tyrosine hydroxylase. *J Neurobiol* **54**, 618-627 (2003).
1016 https://doi.org/10.1002/neu.10185
1017 50 Macpherson, L. J. *et al.* Dynamic labelling of neural connections in multiple colours by
1018 trans-synaptic fluorescence complementation. *Nat Commun* **6**, 10024 (2015).
1019 https://doi.org/10.1038/ncomms10024
1020 51 Waddell, S. Reinforcement signalling in Drosophila; dopamine does it all after all. *Curr*
1021 *Opin Neurobiol* **23**, 324-329 (2013). https://doi.org/10.1016/j.conb.2013.01.005
1022 52 Busto, G. U., Cervantes-Sandoval, I. & Davis, R. L. Olfactory learning in Drosophila.
1023 *Physiology (Bethesda)* **25**, 338-346 (2010). https://doi.org/10.1152/physiol.00026.2010
1024 53 Aso, Y. & Rubin, G. M. Dopaminergic neurons write and update memories with cell-type-
1025 specific rules. *Elife* **5** (2016). https://doi.org/10.7554/eLife.16135
1026 54 Schwaerzel, M. *et al.* Dopamine and octopamine differentiate between aversive and
1027 appetitive olfactory memories in Drosophila. *J Neurosci* **23**, 10495-10502 (2003).
1028 https://doi.org/10.1523/JNEUROSCI.23-33-10495.2003
1029 55 Aso, Y. *et al.* Three dopamine pathways induce aversive odor memories with different
1030 stability. *PLoS Genet* **8**, e1002768 (2012). https://doi.org/10.1371/journal.pgen.1002768
1031 56 Masek, P., Worden, K., Aso, Y., Rubin, G. M. & Keene, A. C. A dopamine-modulated
1032 neural circuit regulating aversive taste memory in Drosophila. *Curr Biol* **25**, 1535-1541
1033 (2015). https://doi.org/10.1016/j.cub.2015.04.027
1034 57 Liu, C. *et al.* A subset of dopamine neurons signals reward for odour memory in
1035 Drosophila. *Nature* **488**, 512-516 (2012). https://doi.org/10.1038/nature11304
1036 58 Burke, C. J. *et al.* Layered reward signalling through octopamine and dopamine in
1037 Drosophila. *Nature* **492**, 433-437 (2012). https://doi.org/10.1038/nature11614
1038 59 Yamagata, N. *et al.* Distinct dopamine neurons mediate reward signals for short- and
1039 long-term memories. *Proc Natl Acad Sci U S A* **112**, 578-583 (2015).
1040 https://doi.org/10.1073/pnas.1421930112
1041 60 Xie, T. *et al.* A Genetic Toolkit for Dissecting Dopamine Circuit Function in Drosophila.
1042 *Cell Rep* **23**, 652-665 (2018). https://doi.org/10.1016/j.celrep.2018.03.068
1043 61 Aso, Y. *et al.* Specific dopaminergic neurons for the formation of labile aversive memory.
1044 *Curr Biol* **20**, 1445-1451 (2010). https://doi.org/10.1016/j.cub.2010.06.048
1045 62 Qi, C. & Lee, D. Pre- and Postsynaptic Role of Dopamine D2 Receptor DD2R in Drosophila
1046 Olfactory Associative Learning. *Biology (Basel)* **3**, 831-845 (2014).
1047 https://doi.org/10.3390/biology3040831
1048 63 Honjo, K., Hwang, R. Y. & Tracey, W. D., Jr. Optogenetic manipulation of neural circuits
1049 and behavior in Drosophila larvae. *Nat Protoc* **7**, 1470-1478 (2012).
1050 https://doi.org/10.1038/nprot.2012.079
1051 64 Boyden, E. S., Zhang, F., Bamberg, E., Nagel, G. & Deisseroth, K. Millisecond-timescale,
1052 genetically targeted optical control of neural activity. *Nat Neurosci* **8**, 1263-1268 (2005).
1053 https://doi.org/10.1038/nn1525

1054 65 Ganguly, A., Qi, C., Bajaj, J. & Lee, D. Serotonin receptor 5-HT7 in Drosophila mushroom
1055 body neurons mediates larval appetitive olfactory learning. *Sci Rep* **10**, 21267 (2020).
1056 https://doi.org/10.1038/s41598-020-77910-5
1057 66 Cognigni, P., Felsenberg, J. & Waddell, S. Do the right thing: neural network mechanisms
1058 of memory formation, expression and update in Drosophila. *Curr Opin Neurobiol* **49**, 51-
1059 58 (2018). https://doi.org/10.1016/j.conb.2017.12.002
1060 67 Owald, D. & Waddell, S. Olfactory learning skews mushroom body output pathways to
1061 steer behavioral choice in Drosophila. *Curr Opin Neurobiol* **35**, 178-184 (2015).
1062 https://doi.org/10.1016/j.conb.2015.10.002
1063 68 Davis, R. L. Olfactory memory formation in Drosophila: from molecular to systems
1064 neuroscience. *Annu Rev Neurosci* **28**, 275-302 (2005).
1065 https://doi.org/10.1146/annurev.neuro.28.061604.135651
1066 69 Aso, Y. *et al.* The neuronal architecture of the mushroom body provides a logic for
1067 associative learning. *Elife* **3**, e04577 (2014). https://doi.org/10.7554/eLife.04577
1068 70 Jefferis, G. S., Marin, E. C., Watts, R. J. & Luo, L. Development of neuronal connectivity in
1069 Drosophila antennal lobes and mushroom bodies. *Curr Opin Neurobiol* **12**, 80-86 (2002).
1070 https://doi.org/10.1016/s0959-4388(02)00293-3
1071 71 Heisenberg, M., Borst, A., Wagner, S. & Byers, D. Drosophila mushroom body mutants
1072 are deficient in olfactory learning. *J Neurogenet* **2**, 1-30 (1985).
1073 https://doi.org/10.3109/01677068509100140
1074 72 de Belle, J. S. & Heisenberg, M. Associative odor learning in Drosophila abolished by
1075 chemical ablation of mushroom bodies. *Science* **263**, 692-695 (1994).
1076 https://doi.org/10.1126/science.8303280
1077 73 Davis, R. L. Traces of Drosophila memory. *Neuron* **70**, 8-19 (2011).
1078 https://doi.org/10.1016/j.neuron.2011.03.012
1079 74 Sejourne, J. *et al.* Mushroom body efferent neurons responsible for aversive olfactory
1080 memory retrieval in Drosophila. *Nat Neurosci* **14**, 903-910 (2011).
1081 https://doi.org/10.1038/nn.2846
1082 75 Owald, D. *et al.* Activity of defined mushroom body output neurons underlies learned
1083 olfactory behavior in Drosophila. *Neuron* **86**, 417-427 (2015).
1084 https://doi.org/10.1016/j.neuron.2015.03.025
1085 76 Zars, T., Fischer, M., Schulz, R. & Heisenberg, M. Localization of a short-term memory in
1086 Drosophila. *Science* **288**, 672-675 (2000). https://doi.org/10.1126/science.288.5466.672
1087 77 Tomchik, S. M. & Davis, R. L. Dynamics of learning-related cAMP signaling and stimulus
1088 integration in the Drosophila olfactory pathway. *Neuron* **64**, 510-521 (2009).
1089 https://doi.org/10.1016/j.neuron.2009.09.029
1090 78 Levin, L. R. *et al.* The Drosophila learning and memory gene rutabaga encodes a
1091 Ca2+/Calmodulin-responsive adenylyl cyclase. *Cell* **68**, 479-489 (1992).
1092 https://doi.org/10.1016/0092-8674(92)90185-f
1093 79 Boto, T., Louis, T., Jindachomthong, K., Jalink, K. & Tomchik, S. M. Dopaminergic
1094 modulation of cAMP drives nonlinear plasticity across the Drosophila mushroom body
1095 lobes. *Curr Biol* **24**, 822-831 (2014). https://doi.org/10.1016/j.cub.2014.03.021

80 Mao, Z. & Davis, R. L. Eight different types of dopaminergic neurons innervate the Drosophila mushroom body neuropil: anatomical and physiological heterogeneity. *Front Neural Circuits* **3**, 5 (2009). https://doi.org/10.3389/neuro.04.005.2009

81 Aso, Y. *et al.* Mushroom body output neurons encode valence and guide memory-based action selection in Drosophila. *Elife* **3**, e04580 (2014). https://doi.org/10.7554/eLife.04580

82 Hartenstein, V., Cruz, L., Lovick, J. K. & Guo, M. Developmental analysis of the dopamine-containing neurons of the Drosophila brain. *J Comp Neurol* **525**, 363-379 (2017). https://doi.org/10.1002/cne.24069

83 Tully, T., Cambiazo, V. & Kruse, L. Memory through metamorphosis in normal and mutant Drosophila. *J Neurosci* **14**, 68-74 (1994). https://doi.org/10.1523/JNEUROSCI.14-01-00068.1994

84 Barnstedt, O. *et al.* Memory-Relevant Mushroom Body Output Synapses Are Cholinergic. *Neuron* **89**, 1237-1247 (2016). https://doi.org/10.1016/j.neuron.2016.02.015

85 Yamada, D., Davidson, A. M. & Hige, T. Cyclic nucleotide-induced bidirectional long-term synaptic plasticity in Drosophila mushroom body. *J Physiol* **602**, 2019-2045 (2024). https://doi.org/10.1113/jp285745

86 Wang, Z. W. Regulation of synaptic transmission by presynaptic CaMKII and BK channels. *Mol Neurobiol* **38**, 153-166 (2008). https://doi.org/10.1007/s12035-008-8039-7

87 Eschbach, C. *et al.* Recurrent architecture for adaptive regulation of learning in the insect brain. *Nat Neurosci* **23**, 544-555 (2020). https://doi.org/10.1038/s41593-020-0607-9

88 Winding, M. *et al.* The connectome of an insect brain. *Science* **379**, eadd9330 (2023). https://doi.org/10.1126/science.add9330

89 Nagarkar-Jaiswal, S. *et al.* A genetic toolkit for tagging intronic MiMIC containing genes. *Elife* **4** (2015). https://doi.org/10.7554/eLife.08469

90 Nagarkar-Jaiswal, S. *et al.* A library of MiMICs allows tagging of genes and reversible, spatial and temporal knockdown of proteins in Drosophila. *Elife* **4** (2015). https://doi.org/10.7554/eLife.05338

91 Lilly, M. & Carlson, J. smellblind: a gene required for Drosophila olfaction. *Genetics* **124**, 293-302 (1990). https://doi.org/10.1093/genetics/124.2.293

92 Varga, S. J., Qi, C., Podolsky, E. & Lee, D. A new Drosophila model to study the interaction between genetic and environmental factors in Parkinson's disease. *Brain Res* **1583**, 277-286 (2014). https://doi.org/10.1016/j.brainres.2014.08.021

93 Qi, C., Varga, S., Oh, S. J., Lee, C. J. & Lee, D. Optogenetic Rescue of Locomotor Dysfunction and Dopaminergic Degeneration Caused by Alpha-Synuclein and EKO Genes. *Exp Neurobiol* **26**, 97-103 (2017). https://doi.org/10.5607/en.2017.26.2.97

94 Xiao, N., Privman, E. & Venton, B. J. Optogenetic control of serotonin and dopamine release in Drosophila larvae. *ACS Chem Neurosci* **5**, 666-673 (2014). https://doi.org/10.1021/cn500044b

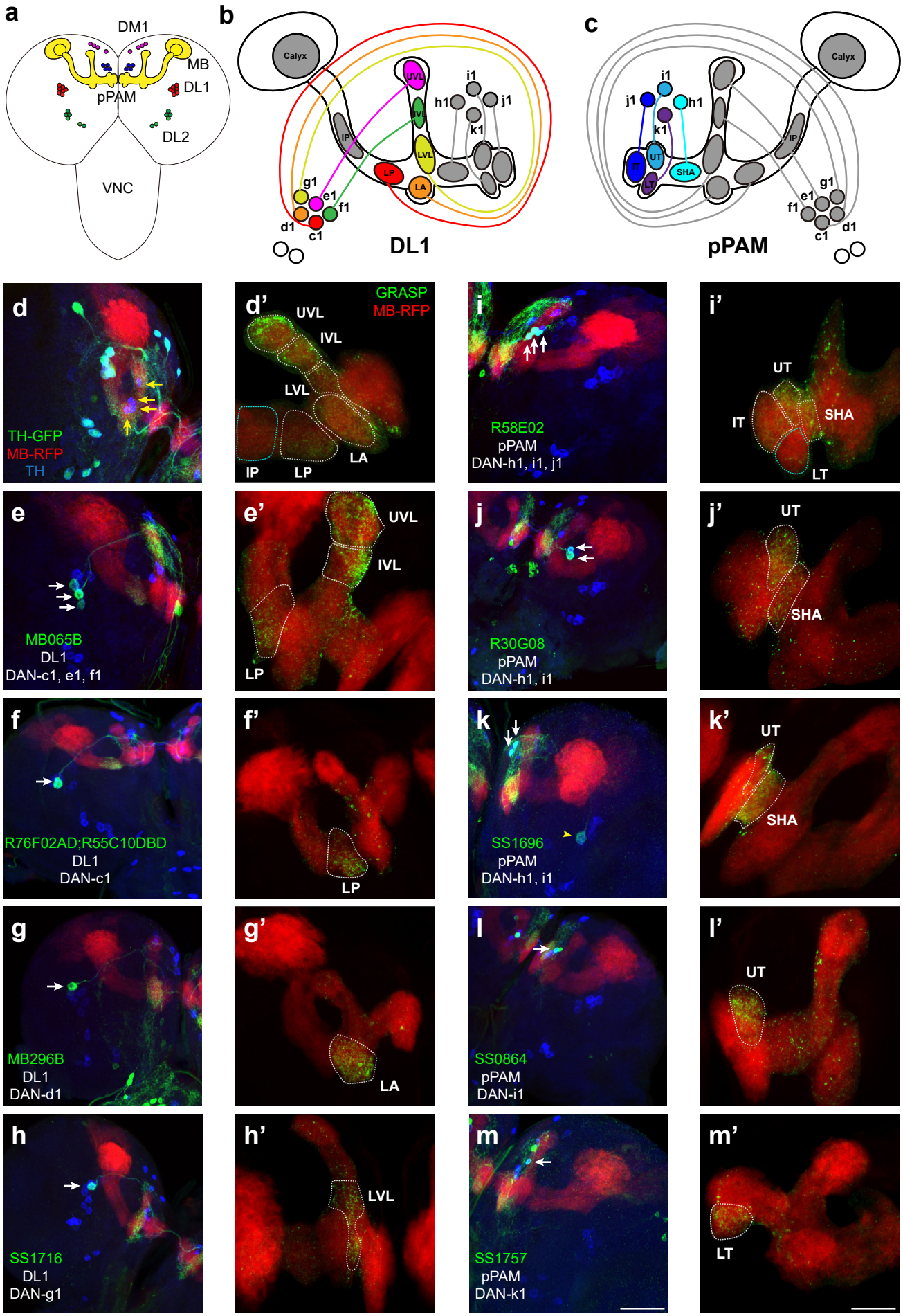
a
DM1
MB
pPAM
DL1
DL2
VNC
b
Calyx
UVL
IVL
LVL
LP
LA
IP
i1
h1
j1
k1
g1
e1
f1
d1
c1
DL1
c
Calyx
i1
j1
h1
k1
IT
UT
LT
SHA
IP
g1
e1
f1
c1
d1
pPAM
d
TH-GFP
MB-RFP
TH
d'
GRASP
MB-RFP
UVL
IVL
LVL
LA
IP
LP
i
R58E02
pPAM
DAN-h1, i1, j1
i'
UT
IT
SHA
LT
e
MB065B
DL1
DAN-c1, e1, f1
e'
UVL
IVL
LP
j
R30G08
pPAM
DAN-h1, i1
j'
UT
SHA
f
R76F02AD;R55C10DBD
DL1
DAN-c1
f'
LP
k
SS1696
pPAM
DAN-h1, i1
k'
UT
SHA
g
MB296B
DL1
DAN-d1
g'
LA
l
SS0864
pPAM
DAN-i1
l'
UT
h
SS1716
DL1
DAN-g1
h'
LVL
m
SS1757
pPAM
DAN-k1
m'
LT

Figure 1

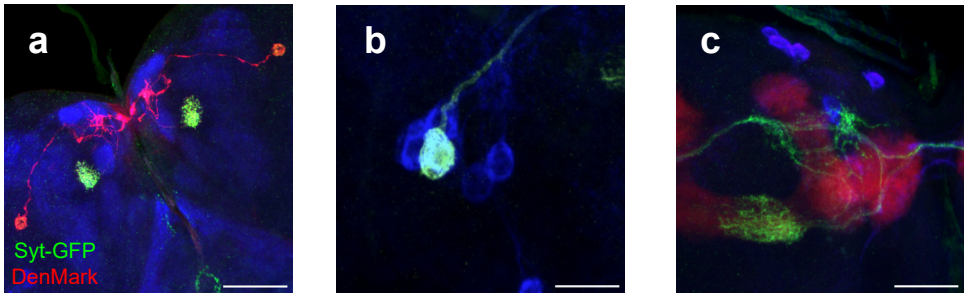
a
Syt-GFP
DenMark
b
c

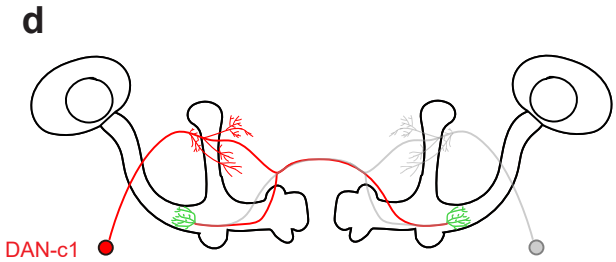
d
DAN-c1

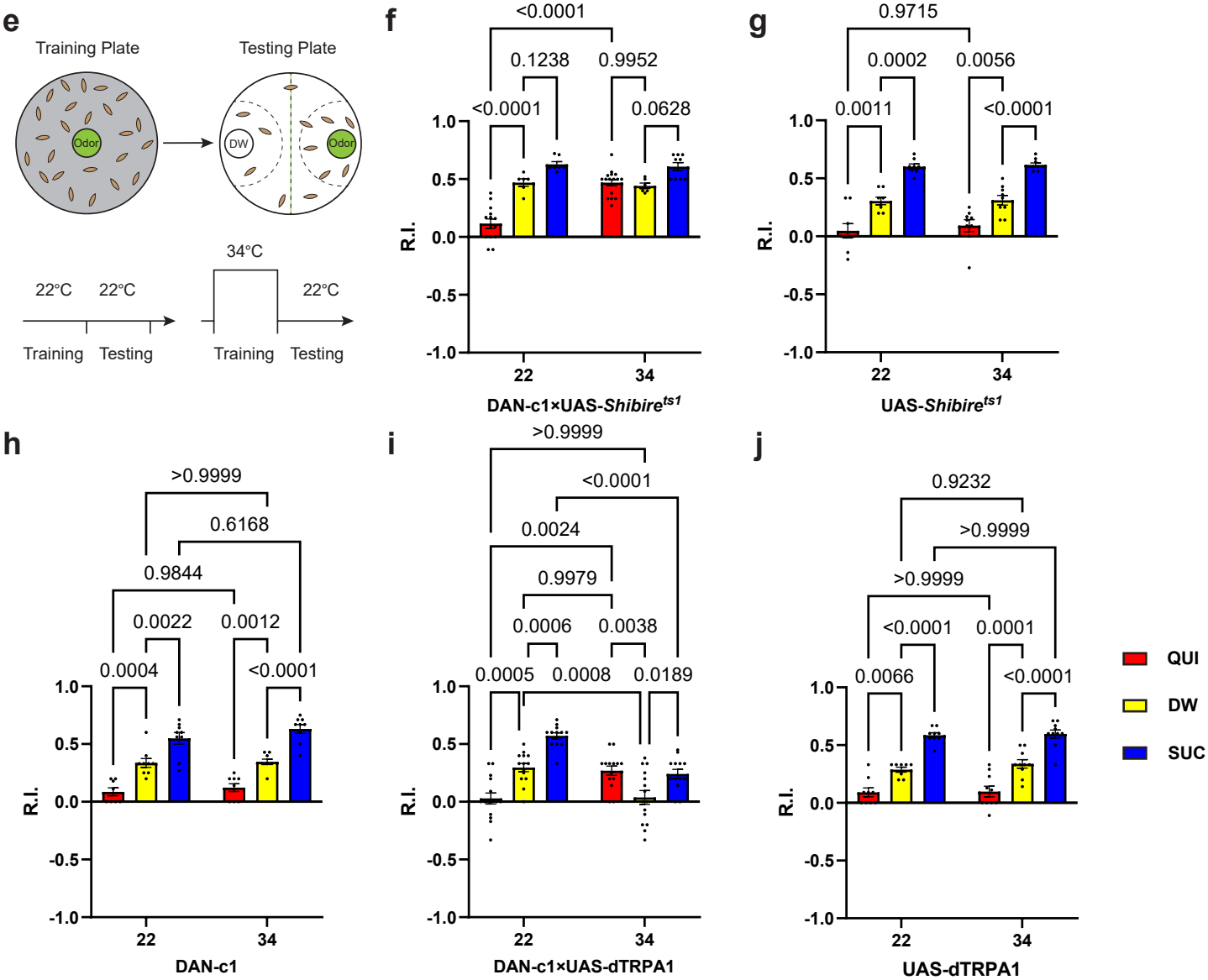
e
Training Plate
Testing Plate
Odor
DW
Odor
22°C
22°C
34°C
22°C
Training
Testing
Training
Testing
f
<0.0001
0.1238
0.9952
<0.0001
0.0628
R.I.
22
34
DAN-c1×UAS-Shibire^ts1
g
0.9715
0.0002
0.0056
0.0011
<0.0001
R.I.
22
34
UAS-Shibire^ts1
h
>0.9999
0.6168
0.9844
0.0022
0.0012
0.0004
<0.0001
R.I.
22
34
DAN-c1
i
>0.9999
<0.0001
0.0024
0.9979
0.0006
0.0038
0.0005
0.0008
0.0189
R.I.
22
34
DAN-c1×UAS-dTRPA1
j
0.9232
>0.9999
>0.9999
<0.0001
0.0001
0.0066
<0.0001
R.I.
22
34
UAS-dTRPA1
QUI
DW
SUC

Figure 2

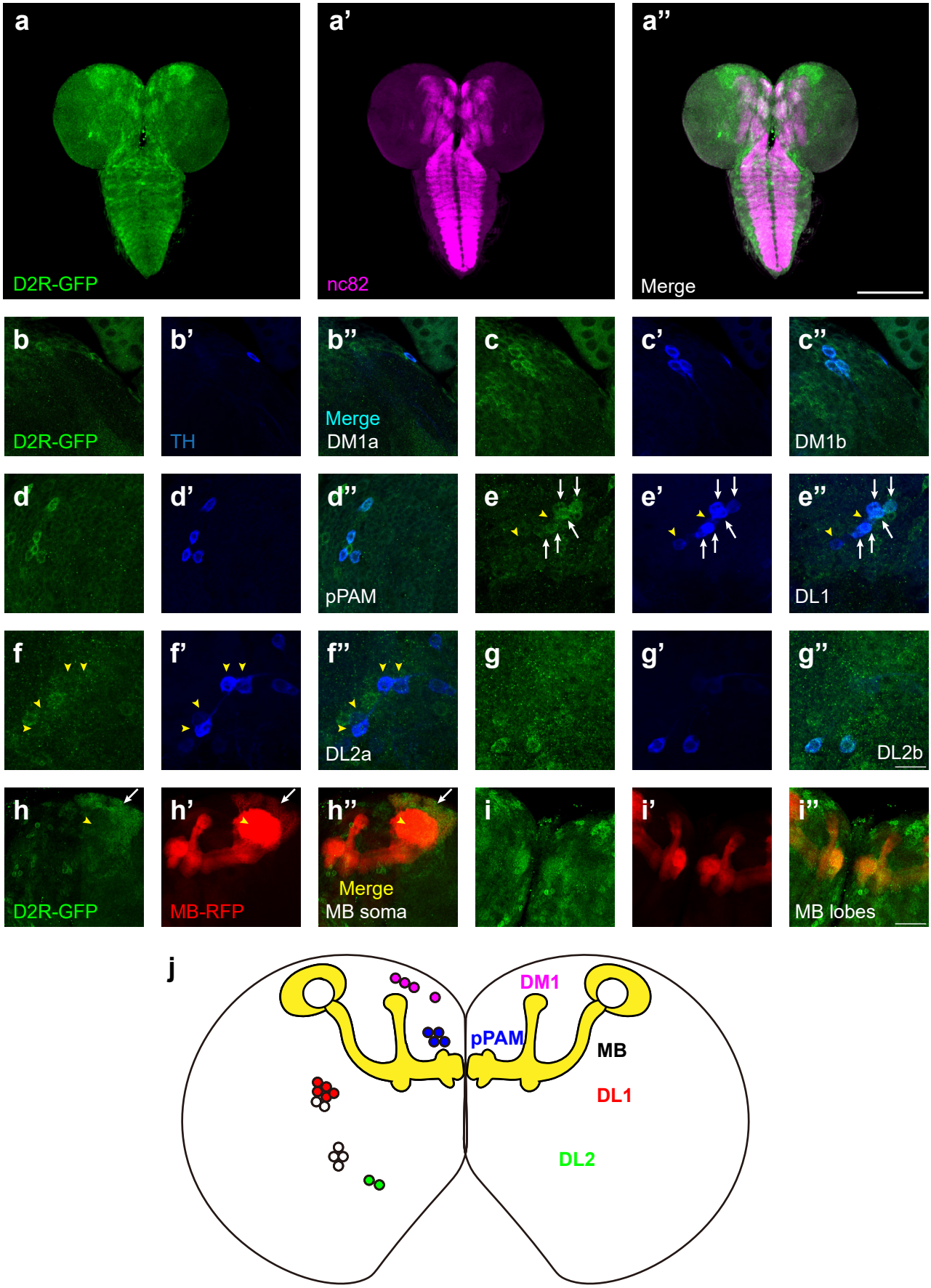
a
D2R-GFP
a'
nc82
a''
Merge
b
D2R-GFP
b'
TH
b''
Merge
DM1a
c
c'
c''
DM1b
d
d'
d''
pPAM
e
e'
e''
DL1
f
f'
f''
DL2a
g
g'
g''
DL2b
h
D2R-GFP
h'
MB-RFP
h''
Merge
MB soma
i
i'
i''
MB lobes
j
DM1
pPAM
MB
DL1
DL2

Figure 3

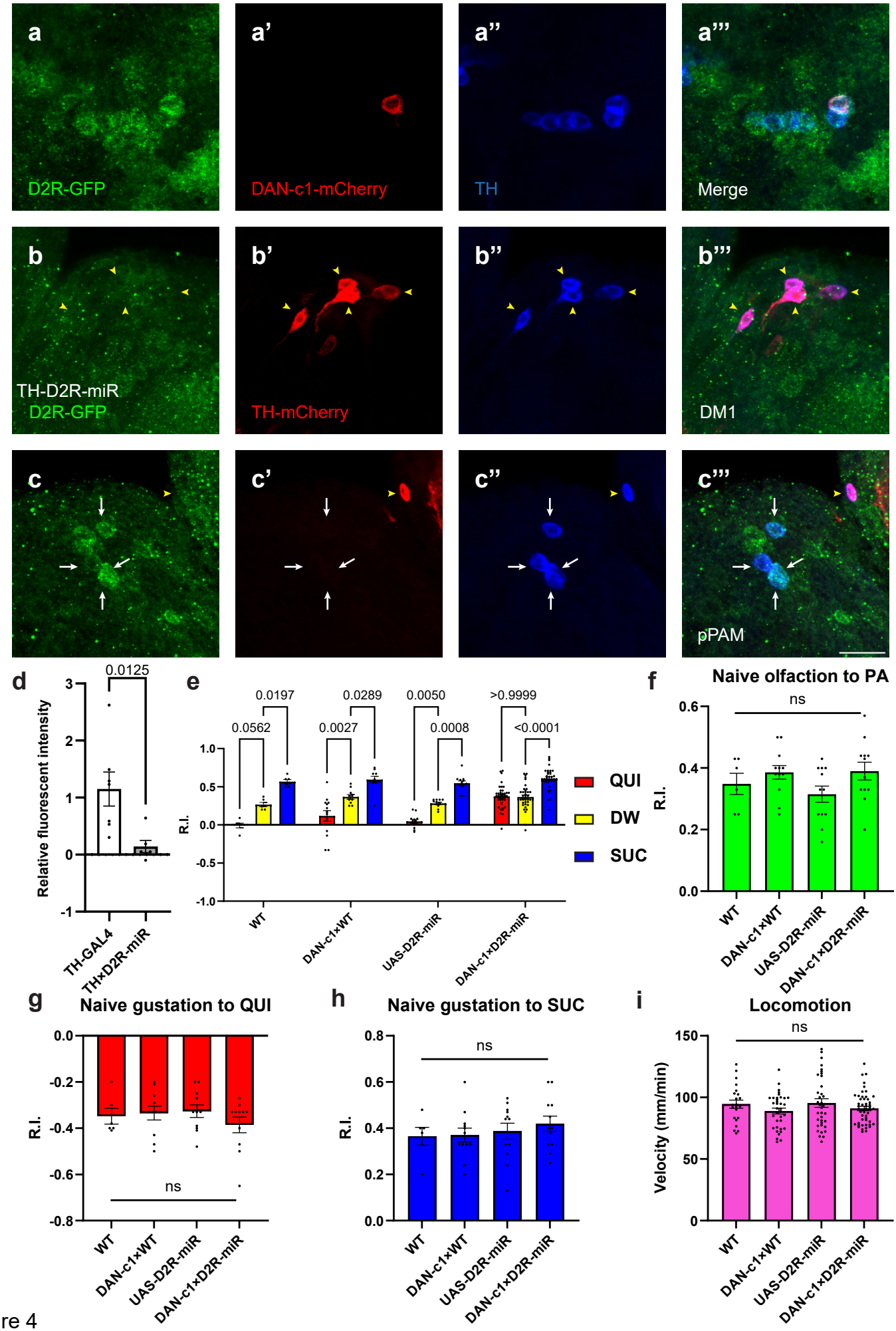
a
D2R-GFP
a'
DAN-c1-mCherry
a''
TH
a'''
Merge
b
TH-D2R-miR
D2R-GFP
b'
TH-mCherry
b''
b'''
DM1
c
c'
c''
c'''
pPAM
d
0.0125
Relative fluorescent intensity
TH-GAL4
TH×D2R-miR
e
0.0562
0.0197
0.0027
0.0289
0.0008
0.0050
<0.0001
>0.9999
R.I.
WT
DAN-c1×WT
UAS-D2R-miR
DAN-c1×D2R-miR
QUI
DW
SUC
f
Naive olfaction to PA
ns
R.I.
g
Naive gustation to QUI
ns
R.I.
h
Naive gustation to SUC
ns
R.I.
i
Locomotion
ns
Velocity (mm/min)

Figure 4

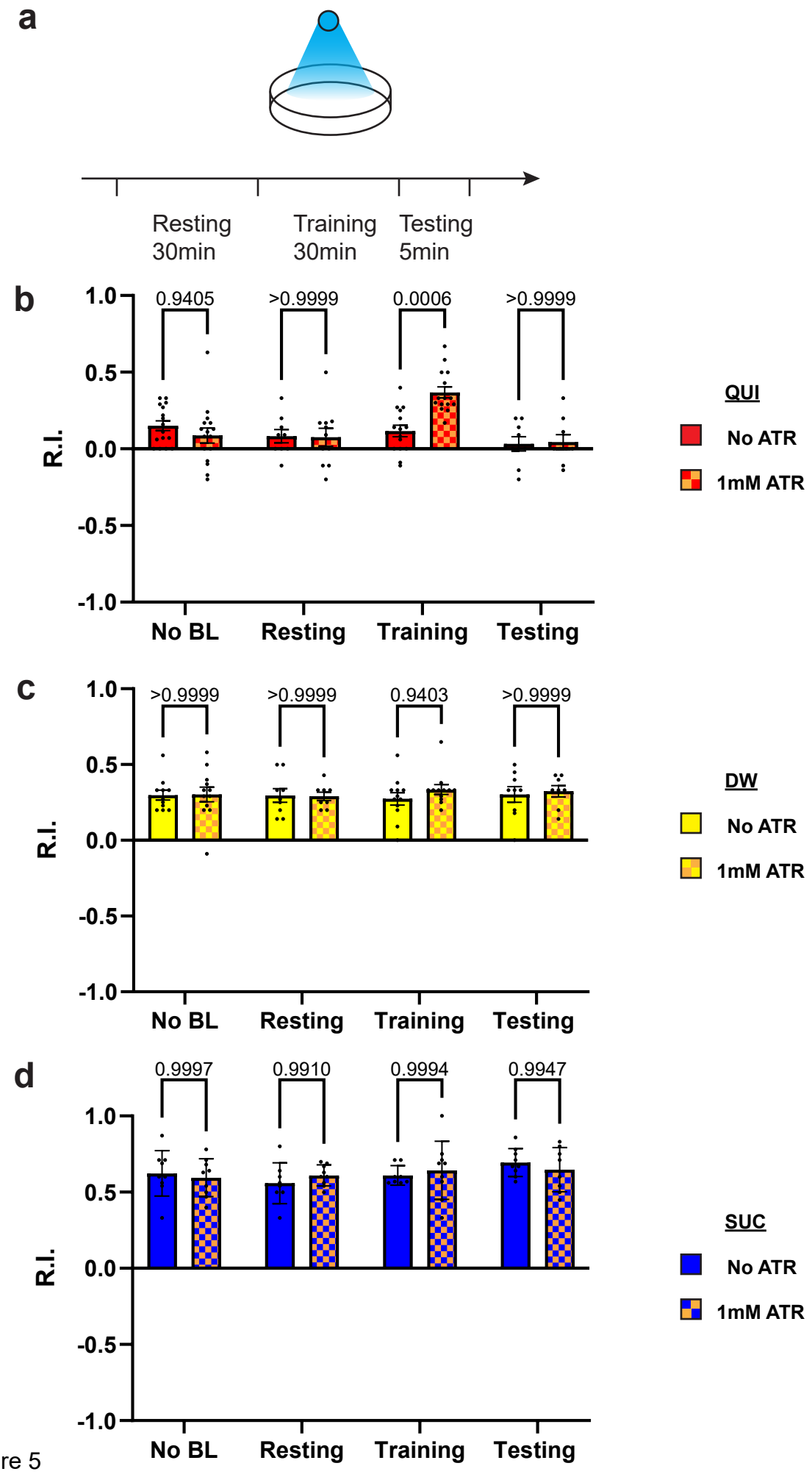
a
Resting
30min
Training
30min
Testing
5min
b
1.0
0.5
0.0
-0.5
-1.0
R.I.
0.9405
>0.9999
0.0006
>0.9999
No BL
Resting
Training
Testing
QUI
No ATR
1mM ATR
c
1.0
0.5
0.0
-0.5
-1.0
R.I.
>0.9999
>0.9999
0.9403
>0.9999
No BL
Resting
Training
Testing
DW
No ATR
1mM ATR
d
1.0
0.5
0.0
-0.5
-1.0
R.I.
0.9997
0.9910
0.9994
0.9947
No BL
Resting
Training
Testing
SUC
No ATR
1mM ATR

Figure 5

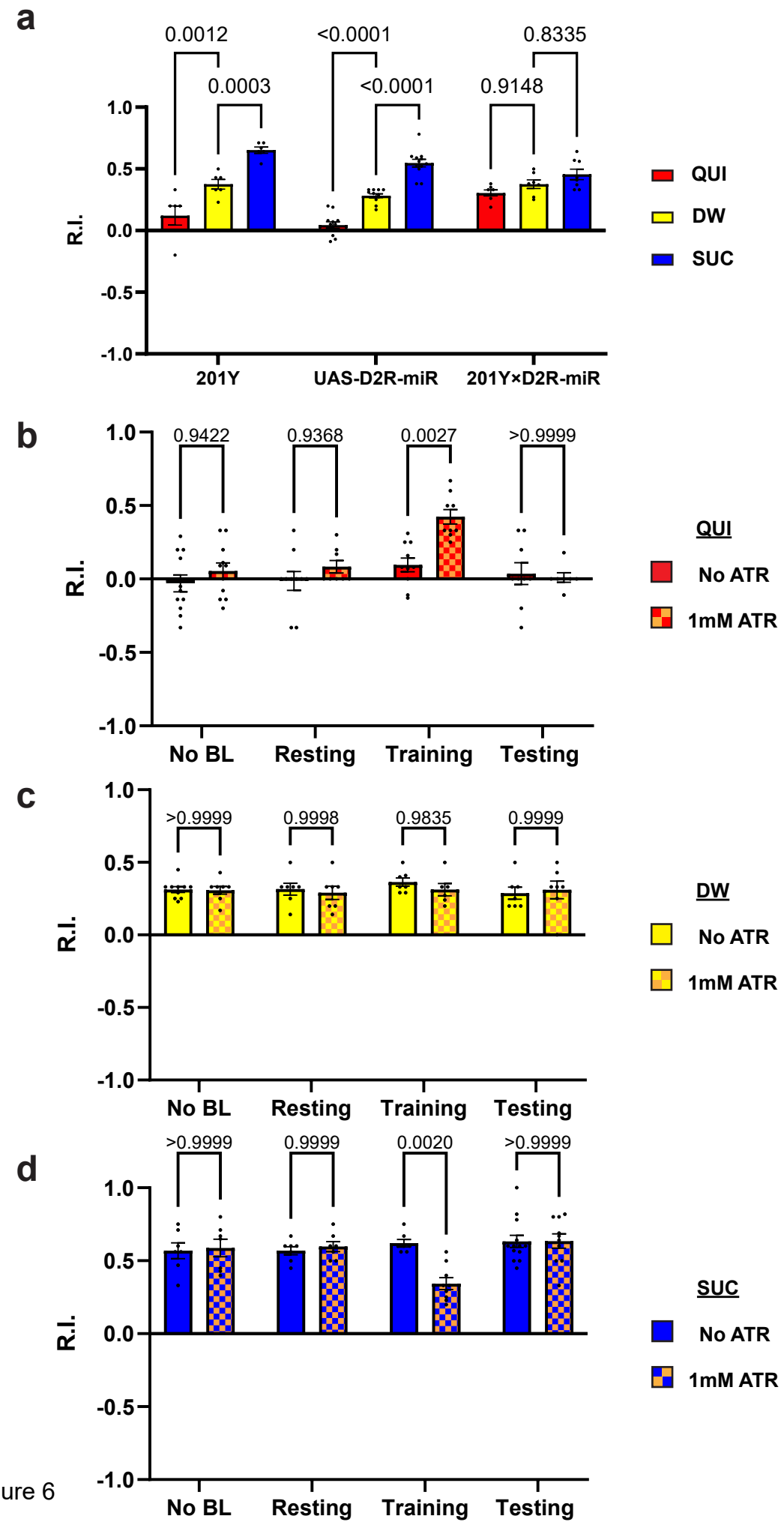
a
0.0012
0.0003
<0.0001
<0.0001
0.8335
0.9148
1.0
0.5
0.0
-0.5
-1.0
R.I.
201Y
UAS-D2R-miR
201Y×D2R-miR
QUI
DW
SUC
b
0.9422
0.9368
0.0027
>0.9999
No BL
Resting
Training
Testing
QUI
No ATR
1mM ATR
c
>0.9999
0.9998
0.9835
0.9999
DW
No ATR
1mM ATR
d
>0.9999
0.9999
0.0020
>0.9999
SUC
No ATR
1mM ATR

Figure 6

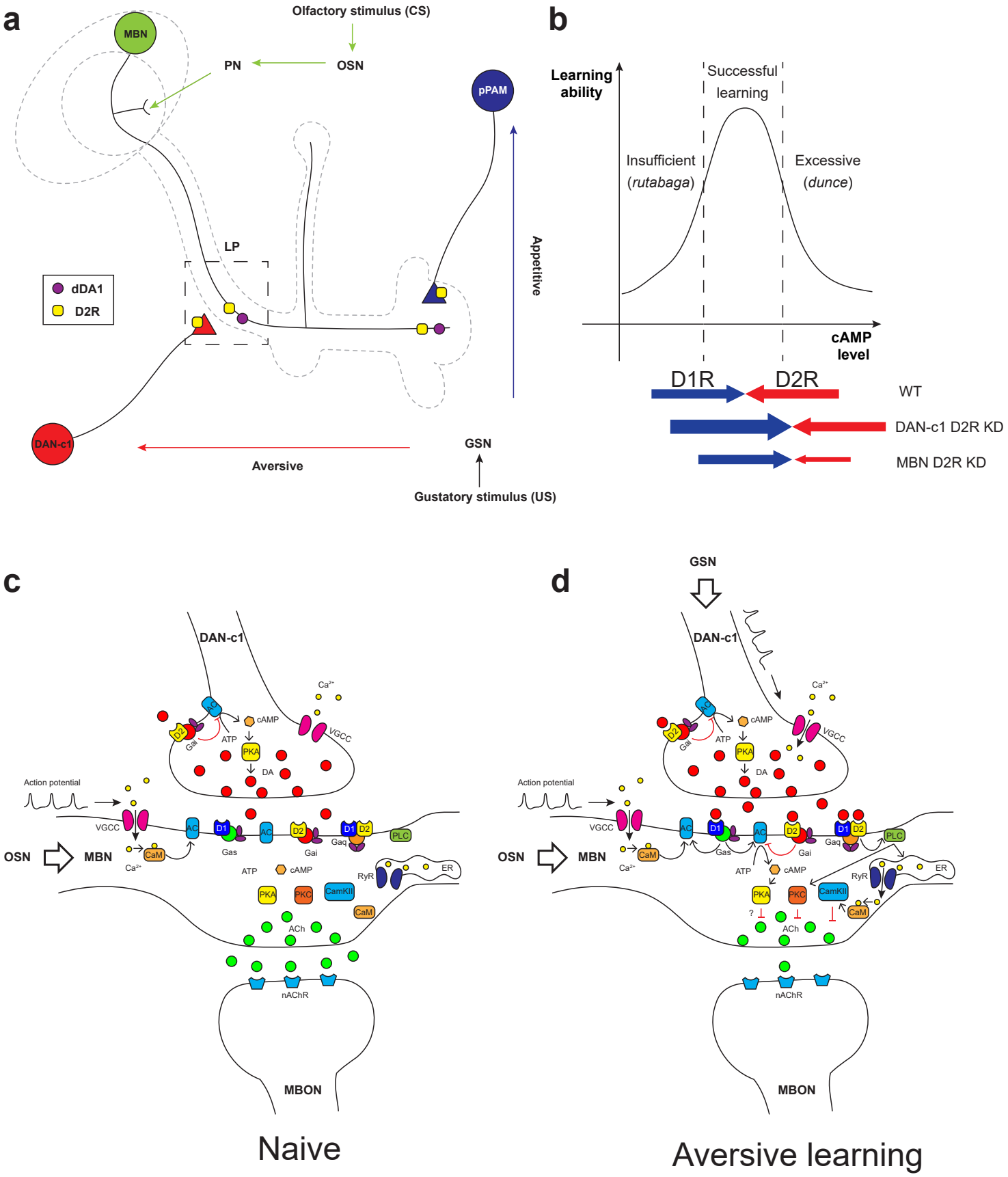
a
Olfactory stimulus (CS)
MBN
PN
OSN
pPAM
LP
dDA1
D2R
Appetitive
DAN-c1
Aversive
GSN
Gustatory stimulus (US)
b
Learning ability
Successful learning
Insufficient (rutabaga)
Excessive (dunce)
cAMP level
D1R
D2R
WT
DAN-c1 D2R KD
MBN D2R KD
c
DAN-c1
Action potential
OSN
MBN
MBON
Naive
d
GSN
DAN-c1
Action potential
OSN
MBN
MBON
Aversive learning

Figure 7

Table 1

	Strains	Name in this work	Neurons in third-instar larval brains		Analogs	Stock #	Source/Gift
			DANs	Non-DANs			
1	TH-Gal4	-	All DANs except pPAM	Some weak	All DANs except PAM (Adult)	-	Dr. J. Hirsh's Lab
2	TH-C'	-	1 DL1, 1 DM1, 3DL2a	Rare	PPL1 + PPM3 (Adult)	-	Dr. M. Wu's lab (Liu et al., 2012)
3	TH-C1	-	-	-	PPL1 + PPM3 (Adult)	-	
4	TH-D'	-	3DL1, 2DL2b	Rare	PPL1 + PPM3 (Adult)	-	
5	TH-D1	-	-	-	PPL1 + PPM3 (Adult)	-	
6	TH-D4	-	-	-	PPL1 + PPM3 (Adult)	-	
7	TH-F1	-	3DL1	Rare	PPL1 + PPM3 (Adult)	-	
8	Th-F2	-	3 DM1, 2-4 DL1, 2DL2a	-	PPL1 + PPM3 (Adult)	-	
9	Th-F3	-	3 DM1b, 1 DL1	-	PPL1 + PPM3 (Adult)	-	
10	TH-G1	-	2-3 DM1, 2-4 DL1, 2 DL2b	-	PPL1 + PPM3 (Adult)	-	
11	R30G08	-	h1, i1, weak k1	-	2 pPAM (L3)	48101	BDSC (Rohwedder et al., 2016)
12	R58E02	-	h1, i1, j1	1	3 pPAM (L3)	41347	
13	R64H06	-	h1, i1, j1, k1	Lots	4 pPAM (L3)	49608	
14	MB315C	-	1-3 pPAM (h1)	Lots	PAM-γ5 (Adult)	-	

15	MB109B	-	-	-	PAM-β'2a, PAM-γ5 (Adult)	-	Janelia Farm (Aso et al., 2014)
16	MB301B	-	-	-	PAM-β'2m, PAM-β2β'2a (Adult)	-	
17	MB056B	-	-	-	PAM-β'2m, PAM-β'2p (Adult)	-	
18	MB032B	-	-	-	PAM-β'2m, PAM-β'2p, PAM-β2β'2a, PAM-γ3 (Adult)	-	
19	MB312B	-	-	-	PAM-γ4, PAM-γ4<γ1γ2 (Adult)	-	
20	MB194B	-	-	-	PAM-α1, PAM-β'2a, PAM-β1, PAM-β1ped, PAM-β2 (Adult)	-	
21	MB063B	-	-	-	PAM-β1 (Adult)	-	
22	MB043B	-	h1, i1, j1	Weak, lots of MBN	PAM-α1, PAM-β'1 ap, PAM-β'1 m, PAM-β1 (Adult)	-	
23	MB441B	-	-	-	PAM-γ3 (Adult)	-	
24	MB025B	-	-	-	PAM-β'1ap/m (Adult)	-	
25	MB438B	-	-	-	PPL1-α'2α2, PPL1-α3, PPL1-γ1pedc (Adult)	-	
26	MB296B	DAN-d1	d1	Some in VNC	PPL1-γ2α'1 (Adult)	-	
27	MB304B	-	-	-	PPL1-α'3 (Adult)	-	

28	MB058B	-	-	-	PPL1-α'2α'2 (Adult)	-	
29	MB065B	-	c1, f1, e1	-	PPL1-α'2α2, PPL1-α'3, PPL1-α3, PPL1-γ2α'1 (Adult)	-	
30	GMR_SS01716	DAN-g1	g1	-	g1 (LVL) (L3)	-	Dr. M. Zlatic's Lab (Saumerber et al., 2018)
31	GMR_SS01696	DAN-h1	h1 + i1	-	h1 (SHA) (L3)	-	
32	GMR_SS00864	DAN-i1	i1	1	i1 (UT) (L3)	-	
33	GMR_SS1757	DAN-k1	k1	1	k1 (LT) (L3)	-	
34	R78E04	-	1 weak DL1	Several	d1 (LA) (L3)	39997	
35	R72B05	-	1 DL1	Lots	MBIN-e2 (L3)	39611	
36	R12C11	-	2 DM1b	Several	MBON-c2 (L3)	76324	
37	R30F04	-	weak d1	Rare	d1 (LA) (L3)	48614	
38	R76C04	-	c1, d1	Rare	c1 (LP) (L3)	48621	
39	R37D06	-	-	-	f1 (IVL) (L3)	47921	
40	R14E06	-	2 DL1	Several	MBIN-e2 (L3)	48643	
41	TH-C-AD;R76F05-DBD	-	1 weak DL1, 2 strong DM1	Lots	PPL1 (SMP-PED) (Adult)	-	Dr. M. Wu's Lab (Xie et al., 2018)
42	TH-F-AD;R61H03-DBD		2DL2, 3 DM1	Rare	PPL1 (SMP) (Adult)	-	
43	R76F02-AD;TH-F-DBD	-	c1, e1	Lots weak	PPL1 (MB-MP1) (Adult)	-	
44	TH-F-AD;R76F05-DBD	-	1 weak DL1, 1-2 strong DM1	Several	PPL1 (SMP-γ) (Adult)	-	
45	R76F02-AD;R60F07-DBD	-	c1, f1, e1	Rare	PPL1 (PED, MB-MP1) (Adult)	-	
46	R60F07-AD;R76F05-DBD	-	g1, e1	Strong SOG	PPL1 (SMP-γ) (Adult)	-	
47	DAT-B-AD;R76F05-DBD	-	2-3pPAM, 1 DL1	Rare	PPL1 (hSMP-γ) (Adult)	-	

48	R76F02-AD;R55C10-DBD	DAN-c1	c1	-	PPL1 (MB-MP1) (Adult)	-	
49	R76F02-AD;R76F01-DBD	-	1 weak DL1	Lots	PPL1 (dFB) (Adult)	-	
50	R76F02-AD;R76F05-DBD	-	-	Lots	PPL1 (dFB) (Adult)	-	
51	R76F05-AD;R61H03-DBD	-	1 DL1, 2 pPAM, 3 DM1	1	PPL1 (MB-MV1) (Adult)	-	
52	WED-1	-	-	-	WED (Adult)	-	Dr. M. Wu's Lab (Liu et al., 2017)
53	WED-2	-	-	-	WED (Adult)	-	
54	TH-FLP/UAS-FRT>>FRT-CD8::GFP;R39G05	-	-	-	PPL1 (bSMP-γ) (Adult)	50063	
55	TH-FLP/UAS-FRT>>FRT-CD8::GFP;R17C11	-	-	-	PPL1 (V1 & MP1) (Adult)	48763	
56	TH-FLP/UAS-FRT>>FRT-CD8::GFP;R39C07	-	2 DL1	-	PPL1 (MV1 & MP1) (Adult)	50039	
57	TH-FLP/UAS-FRT>>FRT-CD8::GFP;R67E08	-	-	-	PPL1 (V1) (Adult)	39445	

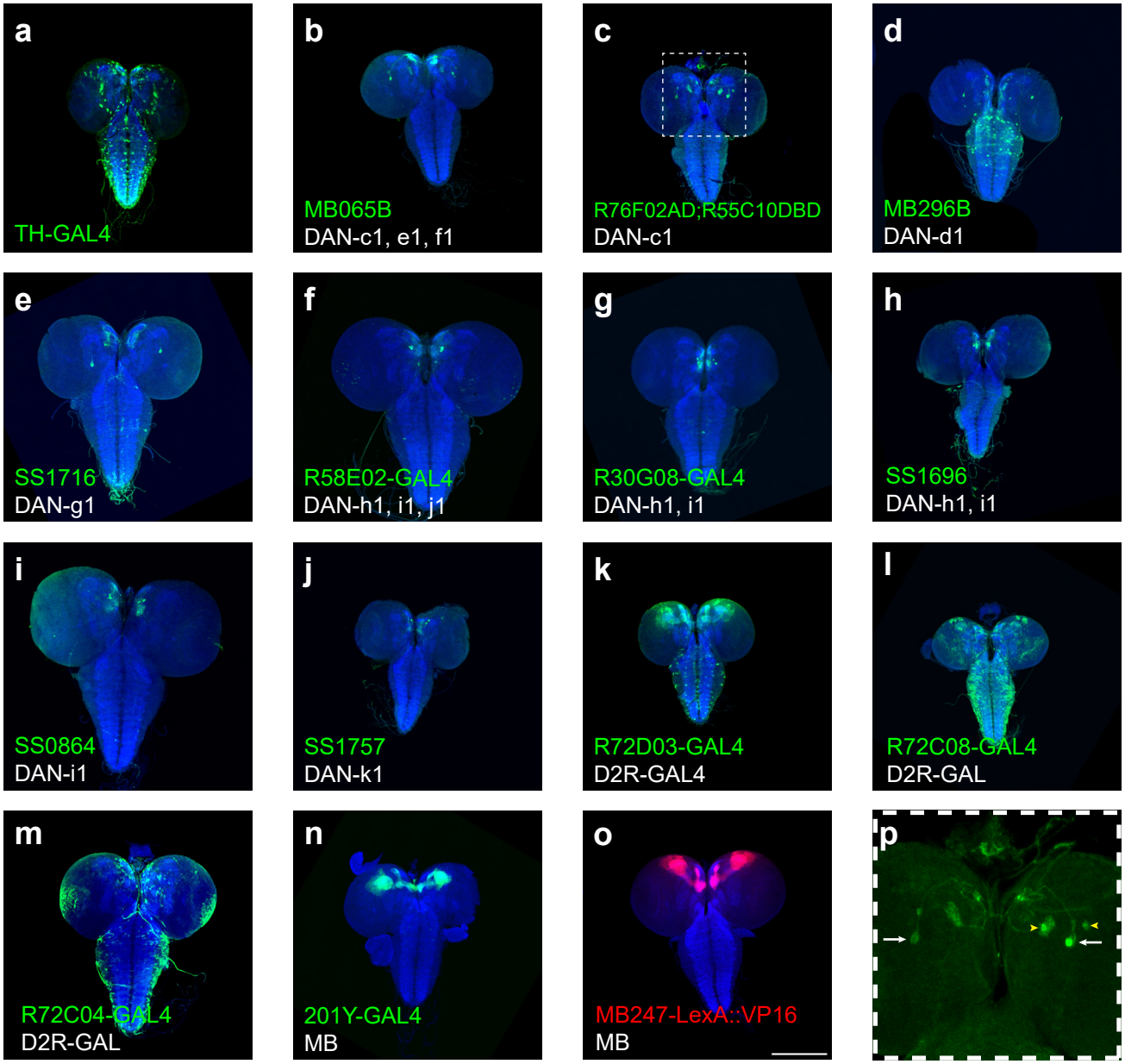
a
TH-GAL4
b
MB065B
DAN-c1, e1, f1
c
R76F02AD;R55C10DBD
DAN-c1
d
MB296B
DAN-d1
e
SS1716
DAN-g1
f
R58E02-GAL4
DAN-h1, i1, j1
g
R30G08-GAL4
DAN-h1, i1
h
SS1696
DAN-h1, i1
i
SS0864
DAN-i1
j
SS1757
DAN-k1
k
R72D03-GAL4
D2R-GAL4
l
R72C08-GAL4
D2R-GAL
m
R72C04-GAL4
D2R-GAL
n
201Y-GAL4
MB
o
MB247-LexA::VP16
MB
p

Figure S1

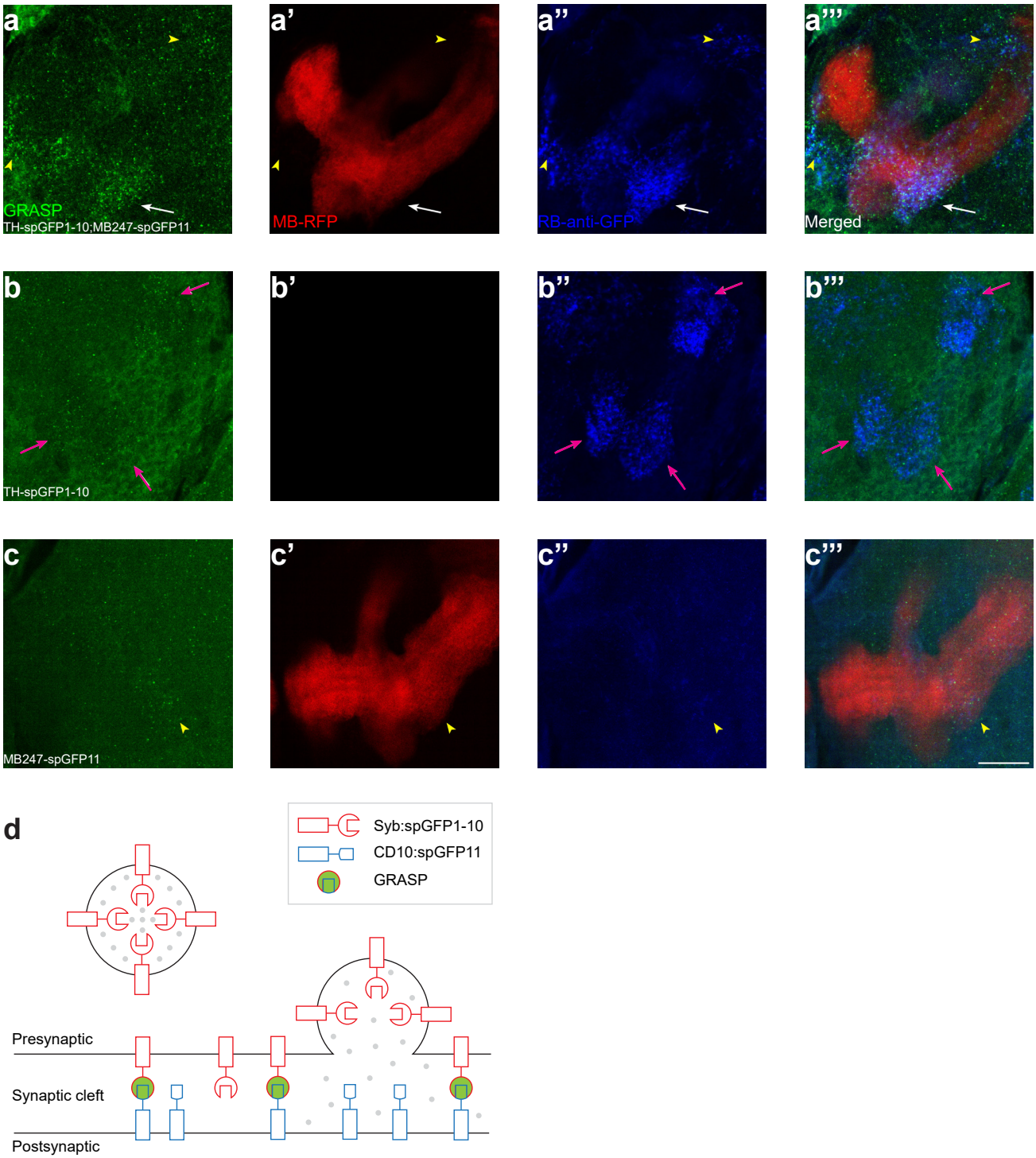
a
GRASP
TH-spGFP1-10:MB247-spGFP11
a'
MB-RFP
a''
RB-anti-GFP
a'''
Merged
b
TH-spGFP1-10
b'
b''
b'''
c
MB247-spGFP11
c'
c''
c'''
d
Syb:spGFP1-10
CD10:spGFP11
GRASP
Presynaptic
Synaptic cleft
Postsynaptic

Figure S2

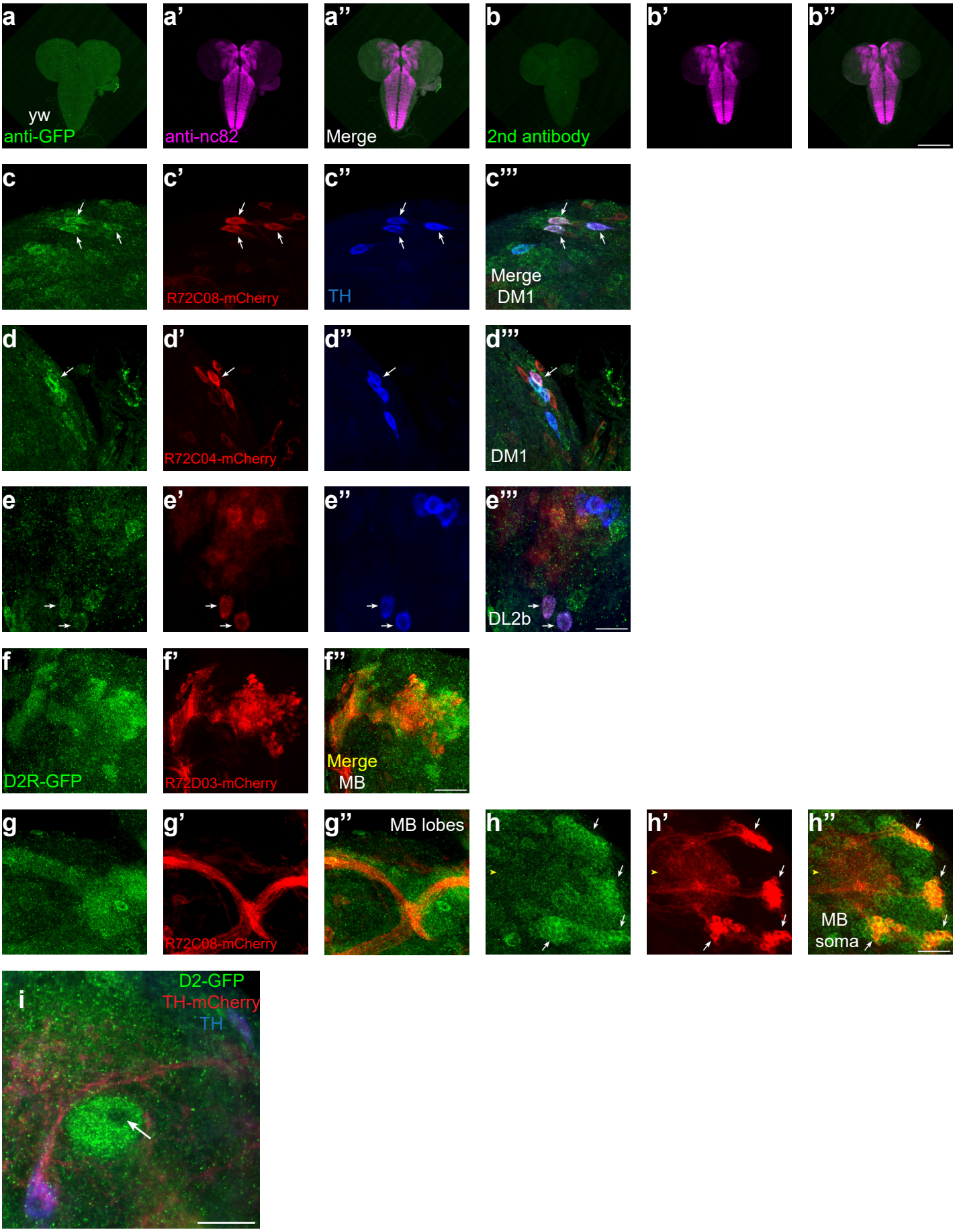
a
yw
anti-GFP
a'
anti-nc82
a''
Merge
b
2nd antibody
b'
b''
c
c'
R72C08-mCherry
c''
TH
c'''
Merge
DM1
d
d'
R72C04-mCherry
d''
d'''
DM1
e
e'
e''
e'''
DL2b
f
D2R-GFP
f'
R72D03-mCherry
f''
Merge
MB
g
g'
R72C08-mCherry
g''
MB lobes
h
h'
h''
MB
soma
i
D2-GFP
TH-mCherry
TH

Figure S3

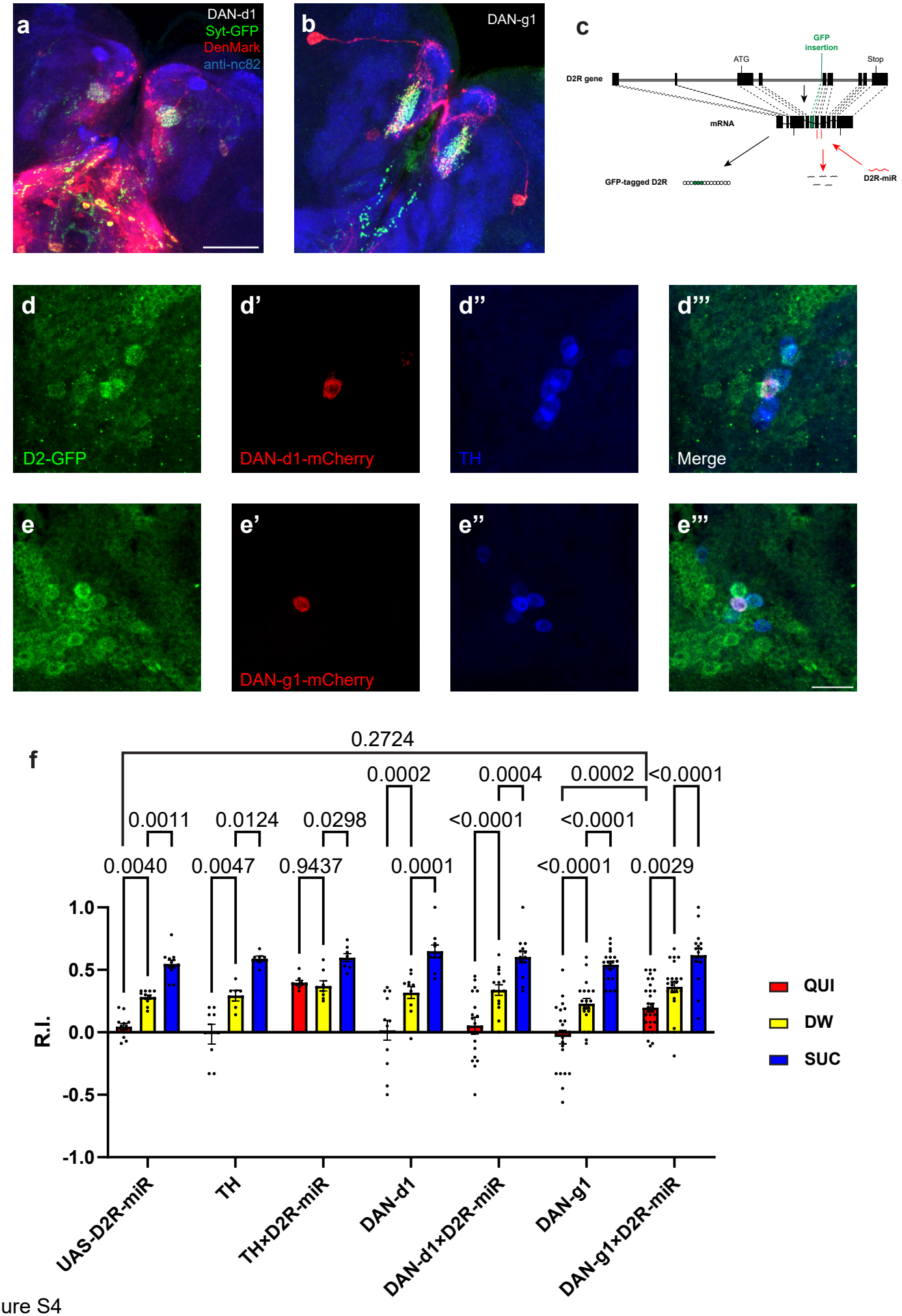
a
DAN-d1
Syt-GFP
DenMark
anti-nc82
b
DAN-g1
c
GFP insertion
ATG
Stop
D2R gene
mRNA
GFP-tagged D2R
D2R-miR
d
D2-GFP
d'
DAN-d1-mCherry
d''
TH
d'''
Merge
e
e'
DAN-g1-mCherry
e''
e'''
f
0.2724
0.0002
0.0004
0.0002
<0.0001
0.0011
0.0124
0.0298
<0.0001
<0.0001
0.0040
0.0047
0.9437
0.0001
<0.0001
0.0029
1.0
0.5
0.0
-0.5
-1.0
R.I.
QUI
DW
SUC
UAS-D2R-miR
TH
TH×D2R-miR
DAN-d1
DAN-d1×D2R-miR
DAN-g1
DAN-g1×D2R-miR

Figure S4

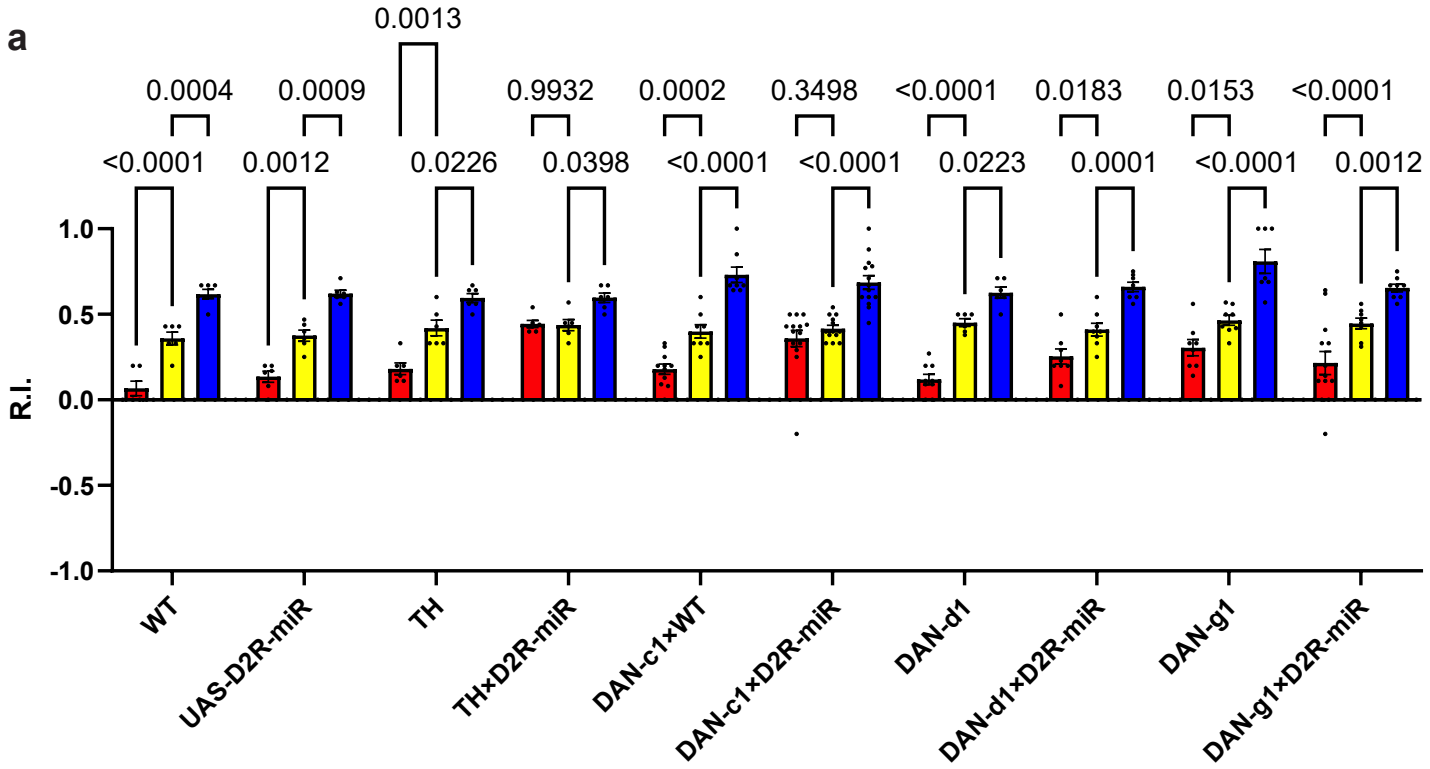
a
0.0013
0.0004
0.0009
0.9932
0.0002
0.3498
<0.0001
0.0183
0.0153
<0.0001
<0.0001
0.0012
0.0226
0.0398
<0.0001
<0.0001
0.0223
0.0001
<0.0001
0.0012
R.I.
1.0
0.5
0.0
-0.5
-1.0
WT
UAS-D2R-miR
TH
TH×D2R-miR
DAN-c1×WT
DAN-c1×D2R-miR
DAN-d1
DAN-d1×D2R-miR
DAN-g1
DAN-g1×D2R-miR

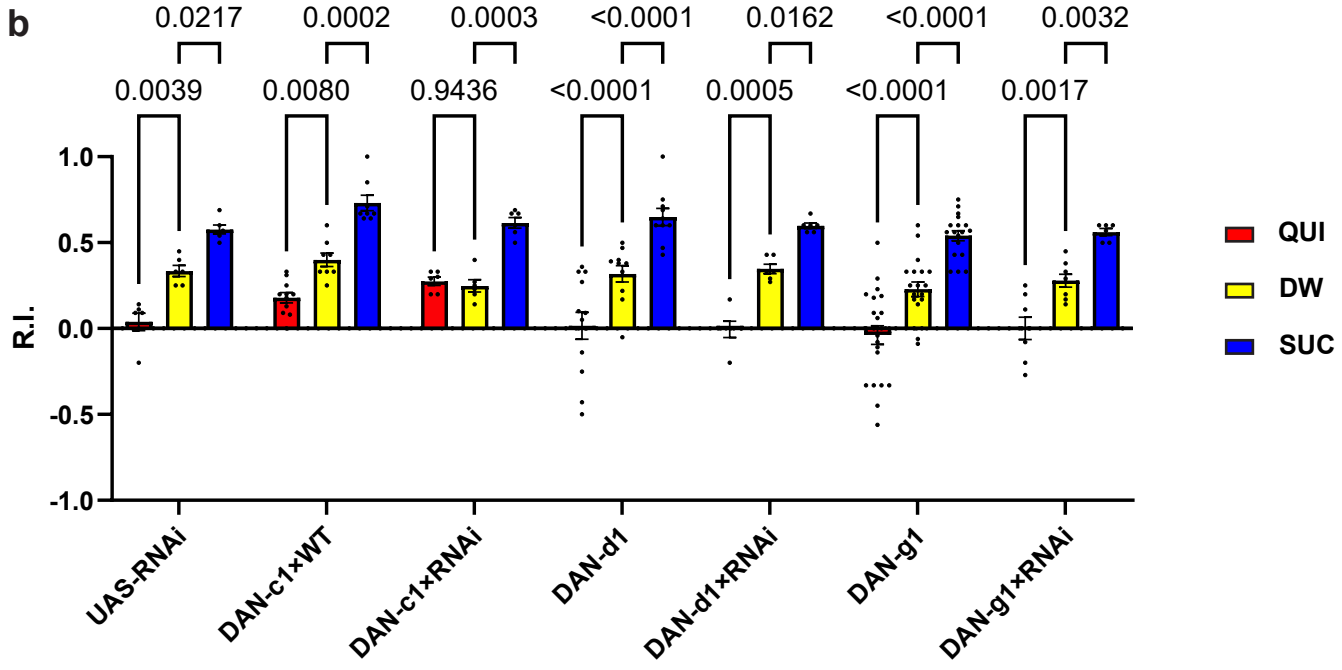
b
0.0217
0.0002
0.0003
<0.0001
0.0162
<0.0001
0.0032
0.0039
0.0080
0.9436
<0.0001
0.0005
<0.0001
0.0017
R.I.
1.0
0.5
0.0
-0.5
-1.0
UAS-RNAi
DAN-c1×WT
DAN-c1×RNAi
DAN-d1
DAN-d1×RNAi
DAN-g1
DAN-g1×RNAi
QUI
DW
SUC

Figure S5

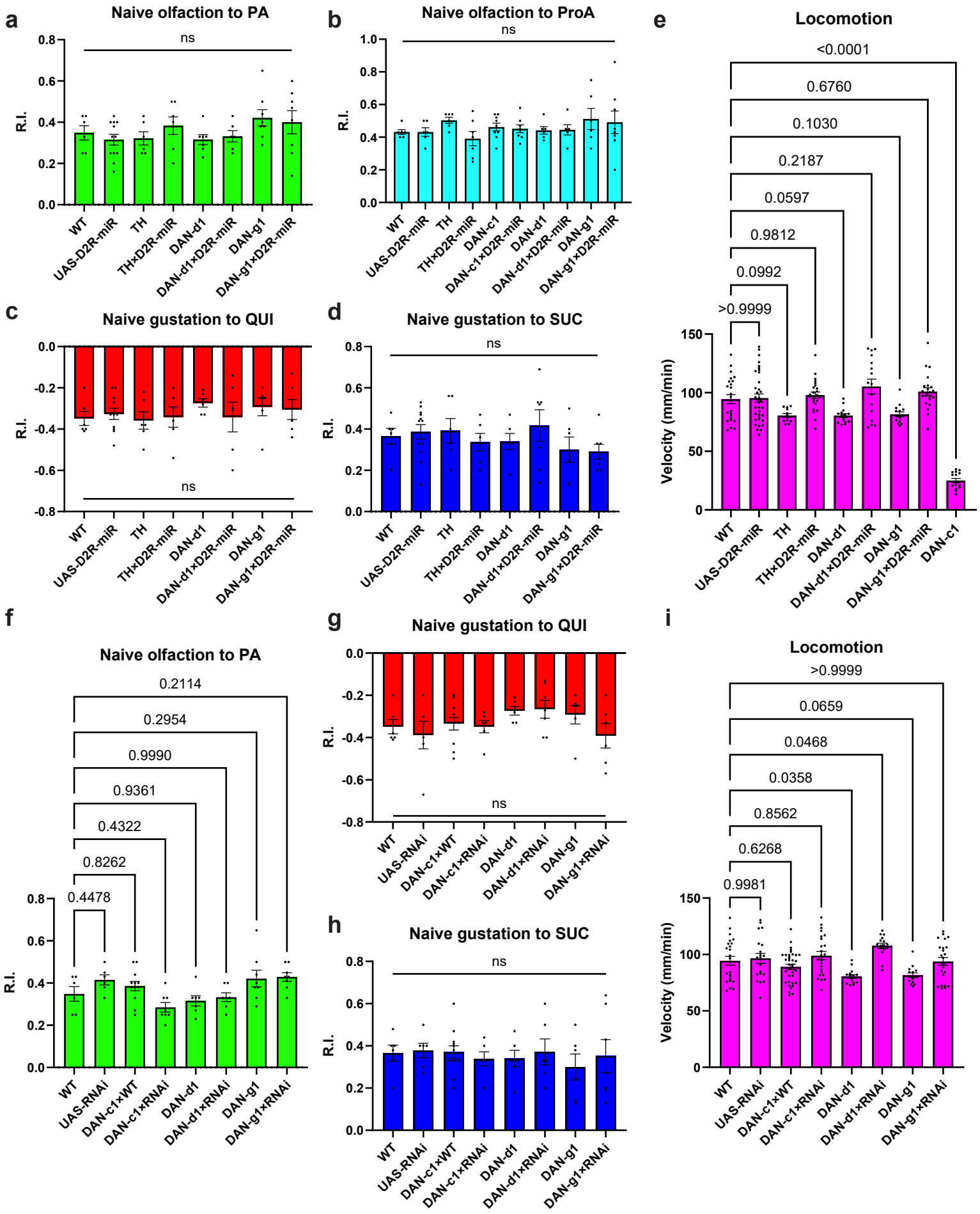
a
Naive olfaction to PA
ns
R.I.
WT
UAS-D2R-miR
TH
TH×D2R-miR
DAN-d1
DAN-d1×D2R-miR
DAN-g1
DAN-g1×D2R-miR
b
Naive olfaction to ProA
ns
R.I.
WT
UAS-D2R-miR
TH
TH×D2R-miR
DAN-c1
DAN-c1×D2R-miR
DAN-d1
DAN-d1×D2R-miR
DAN-g1
DAN-g1×D2R-miR
e
Locomotion
<0.0001
0.6760
0.1030
0.2187
0.0597
0.9812
0.0992
>0.9999
Velocity (mm/min)
WT
UAS-D2R-miR
TH
TH×D2R-miR
DAN-d1
DAN-d1×D2R-miR
DAN-g1
DAN-g1×D2R-miR
DAN-c1
c
Naive gustation to QUI
ns
R.I.
WT
UAS-D2R-miR
TH
TH×D2R-miR
DAN-d1
DAN-d1×D2R-miR
DAN-g1
DAN-g1×D2R-miR
d
Naive gustation to SUC
ns
R.I.
WT
UAS-D2R-miR
TH
TH×D2R-miR
DAN-d1
DAN-d1×D2R-miR
DAN-g1
DAN-g1×D2R-miR
f
Naive olfaction to PA
0.2114
0.2954
0.9990
0.9361
0.4322
0.8262
0.4478
R.I.
WT
UAS-RNAi
DAN-c1×WT
DAN-c1×RNAi
DAN-d1
DAN-d1×RNAi
DAN-g1
DAN-g1×RNAi
g
Naive gustation to QUI
ns
R.I.
WT
UAS-RNAi
DAN-c1×WT
DAN-c1×RNAi
DAN-d1
DAN-d1×RNAi
DAN-g1
DAN-g1×RNAi
h
Naive gustation to SUC
ns
R.I.
WT
UAS-RNAi
DAN-c1×WT
DAN-c1×RNAi
DAN-d1
DAN-d1×RNAi
DAN-g1
DAN-g1×RNAi
i
Locomotion
>0.9999
0.0659
0.0468
0.0358
0.8562
0.6268
0.9981
Velocity (mm/min)
WT
UAS-RNAi
DAN-c1×WT
DAN-c1×RNAi
DAN-d1
DAN-d1×RNAi
DAN-g1
DAN-g1×RNAi

Figure S6

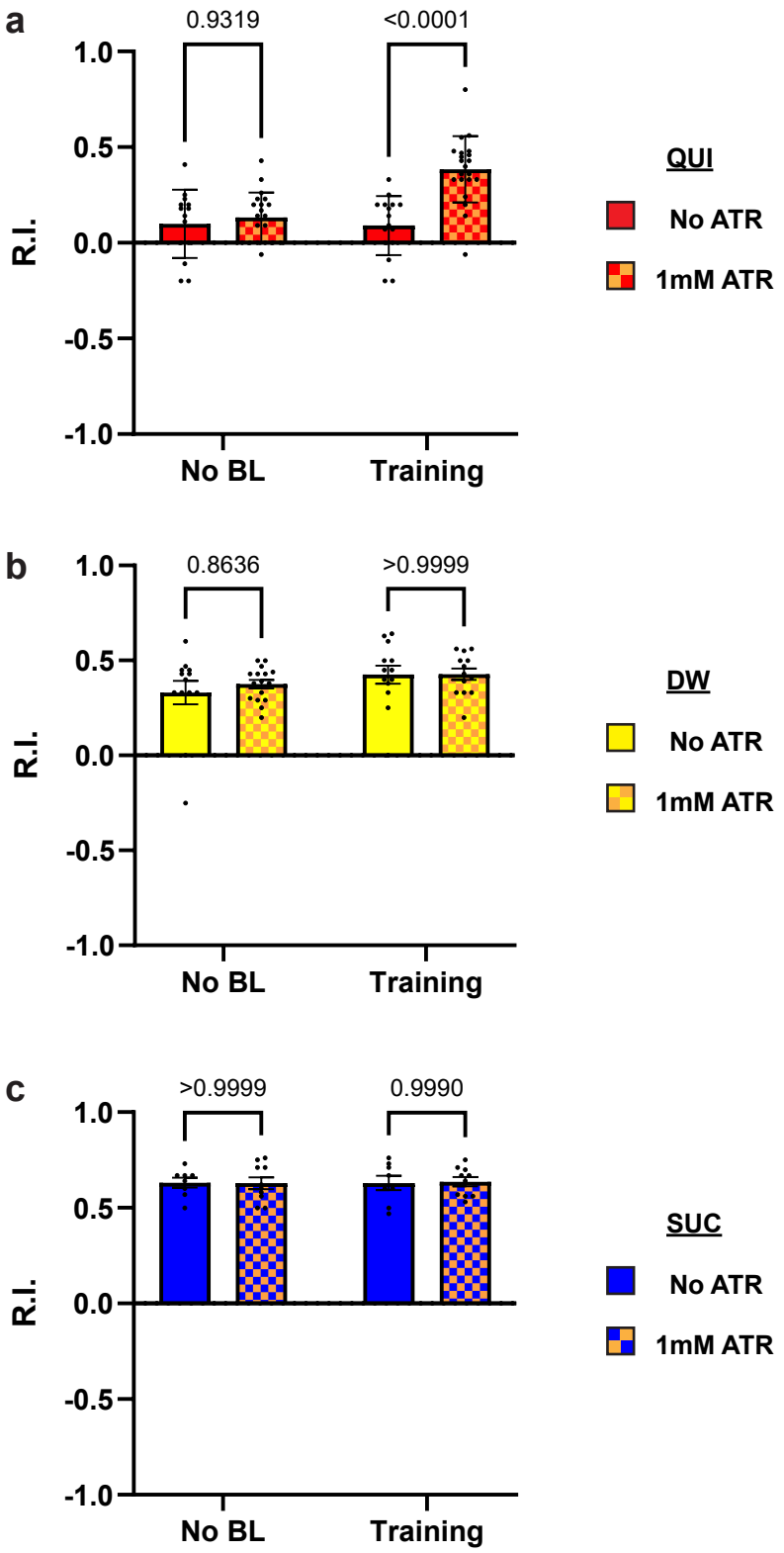
a
0.9319
<0.0001
1.0
0.5
0.0
-0.5
-1.0
R.I.
No BL
Training
QUI
No ATR
1mM ATR
b
0.8636
>0.9999
1.0
0.5
0.0
-0.5
-1.0
R.I.
No BL
Training
DW
No ATR
1mM ATR
c
>0.9999
0.9990
1.0
0.5
0.0
-0.5
-1.0
R.I.
No BL
Training
SUC
No ATR
1mM ATR

Figure S7

Table S1

	Strains	Information	Source/Gift	Stock #
1	R72C04	D2R-GAL4 driver (verified)	BDSC	49416
2	R72C08	D2R-GAL4 driver (verified)	BDSC	49621
3	R72D03	D2R-GAL4 driver	BDSC	46676
4	D2R-EGFP	EGFP-tagged D2R	BDSC	60276
5	201Y-GFP	GFP expressed in Mushroom Body	BDSC	64296
6	MB247-LexA::Vp16/TM6B	MB-LexA, mushroom body driver	Dr. M. Gallio's Lab	Macpherson et al. 2015
7	UAS-nSyb-spGFP1-10,LexAop-CD4-spGFP11/CyO	GRASP strain	BDSC	64314
8	LexAop-nSyb-spGFP1-10,UAS-CD4-spGFP11;MKRS/TM6B	Reverse GRASP strain	BDSC	64315
9	WT(Canton-S)	Wild type	BDSC	64349 (1)
10	UAS-RNAi(D2R) (III) line 2	UAS-D2R-RNAi	Dr. A. Kopin's Lab	Draper et al. 2007
11	201Y-GAL4	MB-GAL4, mushroom body driver	BDSC	4440
12	CyO/Sco;TM2,Ubx/TM6,Hu.Tb	Ballancer Chromesome	Dr. S. Tanda's Lab	
13	1407-Gal4	Pan-neuronal driver	BDSC	8751
14	10XUAS-mCD8::GFP (I)	GFP strain	BDSC	32189
15	10XUAS-mCD8::GFP (II)	GFP strain	BDSC	32186
16	10XUAS-mCD8::GFP (III)	GFP strain	BDSC	32184
17	UAS-ChR2; UAS-ChrR2	Optogenetics strain	Dr. B. Condron's Lab	
18	LexAop-rCD2::RFP; UAS-CD4-spGFP1-10, LexAop-CD4-spGFP11	RFP expressed in MB; GRASP	BDSC	58755
19	UAS-CD8::mCherry (II)	mCherry strain	BDSC	27391
20	UAS-CD8::mCherry (III)	mCherry strain	BDSC	27392
21	yw1118	Wild type for D2R-EGFP	Dr. S. Tanda's Lab	
22	D2R-miR	UAS-DD2R-microRNA	Dr. M. Wu's Lab	Xie et al. 2018
23	UAS-*Shibirets1*	Thermogenetics strain	Dr. T. Kitamoto's Lab	
24	UAS-dTRPA1	Thermogenetics strain	BDSC	26263
25	UAS-nsyb::GFP; UAS-DenMark	Pre- and postsynaptic terminals	BDSC	33056

Table S2

Figure 1	N			Figure S1	N
Strains	**IHC**	**GRASP**		TH-GAL4	4
TH-GAL4	8	16		MB065B	4
MB065B	14	15		R76F02AD;R55C10DBD	5
R76F02AD;R55C10DBD	13	13		MB296B	3
MB296B	14	4		SS1716	2
SS1716	10	21		R58E02	3
R58E02	5	10		R30G08	2
R30G08	13	6		SS1696	4
SS1696	16	4		SS0864	4
SS0864	7	8		SS1757	4
SS1757	6	13		R72D03-GAL4	7
				R72C08-GAL4	5
Figure 2	**N**			R72C04-GAL4	3
DAN-c1 x Syt-GFP;DenMark	4			201Y-GAL4	4
				MB247-LexA::VP16	3
Figure 3	**N**				
DM1a	11			**Figure S2**	**N**
DM1b	9			TH-spGFP1-10	3
pPAM	11			MB247-spGFP11	4
DL1	10				
DL2a	7			**Figure S3**	**N**
DL2b	5			R72D03	5
MB Soma	6			R72C08	4
MB Lobe	8			R72C04	5
Figure 4	**N**			**Figure S4**	**N**
DAN-c1 x D2-GFP	9			DAN-d1 x Syt-GFP;DenMark	6
TH-Gal4	7			DAN-g1 x Syt-GFP;DenMark	3
TH-miR	6			DAN-d1 x D2-GFP	13
				DAN-g1 x D2-GFP	7

Table S3

R76F02AD;R55C10DBD (DAN-c1) brains	other DAN	None DAN	VNC
1	0	1 strong, 4 weak	NA
2	1 weak no neurites	0	3 weak
3	0	7 weak	NA
4	0	0	2 strong
5	0	0	2 strong
6	0	2 strong, 3 weak	NA
7	0	0	NA
8	0	0	4 strong
9	0	5 weak	NA
10	0	1 weak	NA
11	0	8 weak	NA
12	0	0	NA
13	0	4 strong 1 weak	NA
14	0	0	0
15	0	0	0
16	0	0	NA
17	0	0	0
18	NA	1 strong, 1 weak	0
19	NA	7 weak	0
20	NA	5 weak	0
21	NA	0	0
22	NA	1 weak	0

Table S4

	22°C			34°C			Interaction p-value	Row Factor p-value (Temperature)	Column Factor p-value (US)
	QUI	DW	SUC	QUI	DW	SUC			
shibire^{ts1}	9	8	8	9	9	9	0.8880	0.5290	<0.0001
DAN-c1×shibire^{ts1}	14	6	7	17	6	9	<0.0001	0.0018	<0.0001
DAN-c1	8	9	9	9	9	9	0.6143	0.1664	<0.0001
DAN-c1×dTRPA1	15	14	13	14	15	13	<0.0001	0.0019	<0.0001
dTRPA1	9	8	9	10	10	10	0.8001	0.4228	<0.0001

Table S5

Driver	Cross	Pentyl acetate (PA)			Propionic acid (P-A)			Naïve olfactory		Naïve gustatory		Locomotion
		QUI	DW	SUC	QUI	DW	SUC	PA	P-A	QUI	SUC	
TH ×	miR	8	8	8	6	6	6	7	7	6	6	24
	RNAi	-	-	-	-	-	-	-	-	-	-	-
	CR	8	6	6	6	6	6	6	6	6	6	12
DAN-c1 ×	miR	38	38	37	14	13	14	12	8	11	12	50
	RNAi	6	6	6	-	-	-	8	-	6	6	24
	CR	14	10	10	11	8	8	12	9	11	12	36
DAN-d1 ×	miR	17	15	13	8	8	7	6	6	6	7	16
	RNAi	6	6	6	-	-	-	7	-	7	6	16
	CR	13	11	10	9	6	6	7	6	6	6	15
DAN-g1 ×	miR	31	22	16	13	8	8	8	8	6	7	22
	RNAi	8	8	6	-	-	-	8	-	6	7	24
	CR	23	19	18	8	8	7	8	6	6	6	15
201Y ×	miR	7	7	8	6	6	6	6	6	6	6	24
	RNAi	-	-	-	-	-	-	-	-	-	-	-
	CR	6	6	6	6	6	6	6	6	6	6	24
WT		6	6	6	6	6	6	6	6	6	6	24
D2R-miR		12	12	12	6	6	6	12	6	11	12	36
RNAi		6	6	6	-	-	-	6	-	6	6	20

Table S6

Strains	Groups	BL									No BL		
		Resting			Learning			Testing					
		QUI	DW	SUC	QUI	DW	SUC	QUI	DW	SUC	QUI	DW	SUC
TH×ChR2	ATR	-	-	-	21	13	10	-	-	-	20	16	10
	No ATR	-	-	-	16	13	8	-	-	-	14	13	8
DAN-c1×ChR2	ATR	11	8	9	15	12	9	9	8	8	16	11	9
	No ATR	9	9	8	15	12	8	9	9	9	16	12	9
201Y×ChR2	ATR	8	7	7	9	6	9	7	7	10	11	8	7
	No ATR	10	7	7	10	7	7	9	7	13	12	10	7